1   Projecting the futures of plant traits across habitats in Central Europe

2

3   **Running title:** Future projections of plant traits

4

5   Marina Golivets[1*], Sonja Knapp[1,2,3], Franz Essl[4], Bernd Lenzner[4], Guillaume

6   Latombe[5], Brian Leung[6,7], Ingolf Kühn[1,3,8]

7

8   [1]Department of Community Ecology, Helmholtz Centre for Environmental Research – UFZ,
9   Halle, Germany
10   [2]Ecosystem Science/Plant Ecology, Department of Ecology, Technische Universität Berlin,
11   Berlin, Germany
12   [3]German Centre for Integrative Biodiversity Research (iDiv), Halle-Jena-Leipzig, Leipzig,
13   Germany
14   [4]Bioinvasions, Global Change, Macroecology Group, Department of Botany and Biodiversity
15   Research, University of Vienna, Vienna, Austria
16   [5]Institute of Ecology and Evolution, The University of Edinburgh, King's Buildings,
17   Edinburgh, United Kingdom
18   [6]Department of Biology, McGill University, Montreal, Quebec, Canada
19   [7]Bieler School of Environment, McGill University, Montreal, Quebec, Canada
20   [8]Geobotany and Botanical Garden, Martin Luther University Halle-Wittenberg, Halle,
21   Germany
22   [*]Corresponding author

23

24   **Corresponding author:** Marina Golivets, Department of Community Ecology,
25   Helmholtz Centre for Environmental Research – UFZ, Theodor-Lieser-Str. 4,
26   06120, Halle, Germany.
27   Email: maryna.golivets@ufz.de

28

29 ## ABSTRACT

30 Many plant traits covary with environmental gradients, reflecting shifts in

31 adaptive strategies under changing conditions and thus providing information

32 about potential consequences of future environmental change for vegetation

33 and ecosystem functioning. Despite extensive efforts to map trait–environment

34 relationships, the evidence remains heterogeneous and often conflicting,

35 partially because of insufficient consideration of distinct trait syndromes for

36 certain growth forms and habitats. Moreover, it is unclear whether traits of

37 non-native and native plant taxa respond similarly to environmental gradients,

38 limiting our ability to assess the consequences of future plant invasions. Here,

39 using comprehensive data for Germany and the Czech Republic and a Bayesian

40 multilevel modeling framework, we assessed relationships between three major

41 plant traits (maximum height, H_{max}; specific leaf area, SLA; and seed mass, SM)

42 and environmental factors (7 climate variables and percentage of urban land

43 cover) for native and non-native woody and herbaceous plant assemblages

44 across six broad habitat types. We projected the trait change in these

45 assemblages under future environmental change scenarios until 2081–2100 and

46 quantified the change in trait difference between native and non-native plants.

47 Our models depicted multiple trait–environment relationships, with several

48 important differences attributed to biogeographical status and woodiness within

49 and across habitat types. The overall magnitude of trait change is projected to

50 be greater for non-native than native taxa and to increase under more extreme

51 scenarios. Native woody plant assemblages may generally experience an

52   increase across all three traits, whereas woody non-natives may decline in H_{max}

53   and increase in SLA and SM. Herbaceous H_{max} is expected to increase and SLA

54   to decrease in most habitats. The obtained trait projections highlight the

55   conditions under which non-native plants may prevail over natives and vice

56   versa and can serve as a starting point for projecting future changes in

57   ecosystem functions and services.

58

59   **Keywords:** biological invasions, environmental filtering, global environmental

60   change, scenario, trait-based approach, trait–environment relationship

61

62   ## 1 INTRODUCTION

63   Economic globalization and human-induced environmental change over the

64   last centuries have caused vast numbers of species to decline (Díaz et al., 2019),

65   while a smaller yet substantial number of species has expanded beyond their

66   historical ranges (i.e., non-native and neonative species; Essl et al., 2019;

67   Seebens et al., 2017). As a result, previously unique species assemblages around

68   the world are increasingly becoming impoverished, more alike, and less stable

69   (Daru et al., 2021; Eichenberg et al., 2021; Finderup Nielsen et al., 2019; Winter

70   et al., 2009; Yang et al., 2021), with serious, often irreversible, consequences for

71   natural ecosystems and humans (Guo et al., 2020; Naeem et al., 2012; Pyšek et

72   al., 2020). In the face of the highly threatened and uncertain future of

73   biodiversity (Thuiller et al., 2005, 2019), it is important to ensure that the

74   scientific knowledge used to design biodiversity policies is easily updatable,

75   synthesizable, and transferable across space and time. This, on the one hand,

76   calls for approaches that generalize scientific outputs beyond individual species

77   and, on the other hand, requires embracing the distinct ecological patterns

78   displayed by different species groups (e.g., native vs. non-native; Liu et al.,

79   2017).

80   Approaches with a focus on species traits (i.e., any measurable

81   characteristic of a single organism, Violle et al., 2007) are increasingly put

82   forward as a way towards predictive ecology (McGill et al., 2006; Violle et al.,

83   2014) and have been actively employed to study the effects of global

84   environmental change (e.g., Madani et al., 2018; Myers-Smith et al., 2019). The

85   premise of such approaches is that traits mechanistically link an organism's

86   performance to its environment and can be upscaled to understand and predict

87   how the environment shapes species assemblages and ecosystem functioning

88   (Bjorkman et al., 2018; Dubuis et al., 2013; Küster et al., 2011; Lavorel &

89   Garnier, 2002; Musavi et al., 2016). Moreover, traits yield insights into the

90   mechanisms of non-native species invasiveness (Drenovsky et al., 2012; Küster

91   et al., 2008; Pyšek & Richardson, 2008) and can help reveal differences in the

92   ecological roles and functions of native and non-native species (Hulme &

93   Bernard-Verdier, 2018a, 2018b). However, trait differences between natives

94   and non-natives have mostly been assessed independently of the environmental

95   contexts (e.g., Divíšek et al., 2018; Mathakutha et al., 2019; van Kleunen et al.,

96   2010). In contrast, studies that compare how native and non-native traits shift

97   along environmental gradients and therefore allow extrapolating trait

98   differences into different environmental conditions remain scarce (Gross et al.

99   2013; Hanz et al., 2022; Henn et al., 2019; Knapp & Kühn, 2012; Sandel & Low,

100 2019; Westerband et al., 2020). This highlights a mismatch between the trait-

101 based research on native species, which strongly focuses on environmental

102 filtering and adaptation, and that on non-native species, which often

103 insufficiently considers environmental gradients and thus provides only a

104 limited ability to identify the circumstances under which non-natives

105 functionally diverge from or converge with natives.

106   Despite extensive recent efforts to map trait–environment relationships,

107 the evidence on these relationships remains heterogeneous and often

108 discordant. This might be partly attributed to insufficient consideration of

109 distinct trait syndromes specific to different growth forms and habitats.

110 Notably, woody and herbaceous plants occupy distinct sections in the global

111 spectrum of plant form and function (Díaz et al., 2016), which highlights their

112 unique adaptations to the environment and hence divergent trait–environment

113 relationships (Šímová et al., 2018). Additionally, traits of woody species tend to

114 be more strongly associated with climate than those of herbaceous species

115 (Šímová et al., 2018). This suggests that when all growth forms in a study area

116 are jointly analyzed, trait–environment relationships may appear weak.

117 Nevertheless, it is a common practice for macroecological analyses to pool trait

118 data for woody and herbaceous species together (e.g., Boonman et al., 2020;

119 Moles et al., 2009, 2014; Ordonez et al., 2009; Wright et al., 2005) or to focus

120 only on woody taxa (e.g., Šímová et al., 2015; Swenson et al., 2012), thus

121 hindering generalizations of trait–environment relationships. Moreover, the

122 strength and direction of the associations between traits and environment may

123 vary across different environmental conditions such as represented by habitat

124 types. Most frequently, however, trait–environment relationships have been

125 quantified either as pooled across habitats or for a single specific habitat type

126 per study (e.g., montane open habitats, Dubuis et al., 2013; forests, Maes et al.,

127 2020; Wieczynski et al., 2019). For non-native species, habitat information has

128 been primarily incorporated to compare the levels of invasion across broadly

129 defined (Chytrý et al., 2008) and selected narrowly defined (e.g., grasslands,

130 Axmanová et al., 2021; coastal dunes, Giulio et al., 2020; forests, Wagner et al.,

131 2017) habitats, whereas how traits of non-native species arrange along

132 environmental gradients within or across habitats has not been explored.

133 Collectively, this calls for an explicit consideration of woodiness, habitat type,

134 as well as biogeographical status in trait-based analyses.

135   In this study, we used extensive plant distribution and trait data for

136 Germany and the Czech Republic and a full Bayesian multilevel modeling

137 framework to assess future trait change following the "assemble first, predict

138 later" approach (Ferrier & Guisan, 2006). We (1) quantified relationships of

139 traits central to plant life history (Díaz et al., 2016; Westoby, 1998) – namely,

140 maximum height, specific leaf area, and seed mass – with climate and land use

141 within native and non-native plant assemblages. Based on obtained trait–

142 environment relationships, we (2) determined the magnitude and direction of

143 plausible future change in mean trait values, which reflect the turnover of taxa

144 and associated functions. The trait change was projected under seven combined

145 climate and socio-economic scenarios for Europe for the period of 2081–2100.

146 Considering the substantial variation in plant adaptive strategies across growth

147 forms and environments, which may weaken or bias the environmental

148 filtering signal if not accounted for (Catford et al., 2021), we addressed each of

149 the goals separately for woody and herbaceous plants and for species pools of

150 six different broad habitat types.

151

152 ## 2 MATERIAL AND METHODS

153 ### 2.1 Study area

154 Our study area comprises the entire territory of two Central European

155 countries, Germany and the Czech Republic. Both countries are characterized

156 by a temperate climate with marked regional differences. Mean annual

157 temperature (MAT) ranges from *c.* 4 °C at high elevations to 11 °C in the

158 lowlands, being on average *c.* 8 °C. Total annual precipitation (TAP) averages at

159 700 mm, ranging from 450 mm in north-eastern lowlands and the east to 1200

160 mm in the south (Alps) and west (DWD, 2017). Land cover composition across

161 the study area is represented by arable land (37–38%; as of 2018), forested land

162 (30–35%), pastures and mosaic farmland (18–20%), artificial surfaces (7–9%),

163 and semi-natural non-forested land including wetlands and water bodies (1–

164 4%) (EEA, 2021). The sprawl of artificial surface areas has been the main driver

165   of land-use change over the past two decades in Germany, whereas in the

166   Czech Republic land-use change has been primarily marked by the expansion

167   of forested land (EEA, 2021). For Germany, an increase in MAT by 2.8–5.2 °C

168   and either a decrease or increase in TAP by up to 26% in 2071–2100 (compared

169   to 1971–2000) is projected under severe climate change (RCP8.5) (DWD, 2018).

170   For the Czech Republic, MAT is projected to increase by 4.1 °C and TAP – by

171   up to 16% in 2081–2100 (relative to 1981–2010) under RCP8.5 (Český

172   hydrometeorologický ústav, 2019). Climate change is expected to lead to more

173   frequent extreme drought and rainfall events (Huang et al., 2015; Rulfová et al.,

174   2017; Štěpánek et al., 2016) and increased heatwave impacts (e.g., Krkoška

175   Lorencová et al., 2018) in the study area, among other effects.

176

2.2 Data

Taxon-level data

179   Using multiple open data sources, we collated data on plant taxon occurrences,

180   biogeographical status, habitat affinity, and traits for the entire flora of the

181   study area. We excluded aquatic (i.e., taxa with the Ellenberg moisture

182   indicator value >9), holoparasitic, and fully mycotrophic taxa from analyses.

183   *Occurrence records.* For Germany, we obtained grid-based native and alien

184   plant taxon occurrence data from the FlorKart database (Datenbank FlorKart,

185   NetPhyD & BfN, 2013) via the information online system FloraWeb

186   (www.floraweb.de; accessed 5 February 2022). FlorKart is the most

187   comprehensive database on plant taxon distribution for Germany, being the

188   result of the combined effort of thousands of volunteers, who were involved in

189   floristic mapping and literature review. From the FlorKart data, which provided

190   the status of each occurrence record, we excluded records of cultivated,

191   erroneous, and doubtful occurrences. For the Czech Republic, we obtained

192   grid-based taxon presence data (i.e., a single record per taxon per grid cell) from

193   the Pladias – Database of the Czech Flora and Vegetation (www.pladias.cz;

194   accessed 16 January 2022). The database resulted from the integration of over

195   13 million records of *c.* 5,000 species, which originated from multiple national

196   and regional projects, as well as additional data collection efforts within the

197   Pladias project; it is the most complete database on vascular plant occurrence in

198   the Czech Republic (Chytrý et al., 2021; Wild et al., 2019). From the Pladias

199   data, we initially excluded records at the genus level. Records of presently

200   missing or extinct taxa were also removed. Additionally, we excluded data for a

201   few taxa that were known to occur in both countries but for which data were

202   available from a single country only.

203   The FlorKart and Pladias data were provided at the resolution of the 10'

204   longitude × 6' latitude grid cells (corresponding to *c.* 12.0 km × 11.1 km on the

205   50th parallel). Grid cells in both datasets were originally defined by the sheets

206   (tiles) on the German topographical map (Messtischbla□tter) with a scale of

207   1:25000 (TK 25), which is commonly used for floristic mapping. Because both

208   databases are essentially compilations of many regional projects with different

209   sampling intensities, we aggregated all data at the grid-cell level ($N = 3,569$) to

210   achieve a more homogeneous sampling effort across the study area. We also

211   cropped the spatial grid to the combined borders of Germany and the Czech

212   Republic and excluded all grid cells with a land area <117 km², which

213   corresponds to the size of the smallest grid cell not truncated by borders or

214   coastlines. To further control for the differences in sampling effort, we

215   excluded grid cells containing less than 83 of the 87 benchmark taxa.

216   Benchmark taxa were taxa that based on the Beals smoothing method (Beals,

217   1984; Carmona & Pärtel, 2021) occurred in each grid with a probability >0.98.

218   These taxa were determined after all taxonomic names were standardized (see

219   below) and taxa that did not meet the selection criteria (e.g., casual non-natives;

220   see below) were removed. The final grid comprised 3,031 cells, of which 2,481

221   were located majorly (i.e., >50% of grid cell area) in Germany and 550 in the

222   Czech Republic. As grid cells were delineated by geographic minutes, their size

223   varied with latitude from 117 (in the north) to 139.7 km² (in the south).

224   *Biogeographical status.* For Germany, we mostly relied on the information on

225   the origin (native, non-native), introduction time (archaeophyte, i.e.,

226   introduced before the discovery of the Americas in 1492; neophyte, i.e.,

227   introduced after the discovery of the Americas), and establishment status

228   (established, casual, cultivated) from the BiolFlor database (Kühn et al., 2004)

229   and FloraWeb (www.floraweb.de). In case of discrepancies or missing

230   information, we also checked other sources (e.g., Flora Germanica, www.flora-

231   germanica.de), giving preference to local and/or more recent evidence. For the

232   Czech Republic, we used the status information from Pyšek et al. (2012). Using

233   the information on the taxon status, we filtered plant distribution data.

234   Specifically, for taxa that were native in one country and casual non-native in

235   the other country, we retained only records from where those taxa were native.

236   Likewise, for taxa that were native or established non-native in one country but

237   known solely from cultivation in the other country, we considered only data

238   from where those taxa were established. For non-natives that occurred in both

239   countries but were established in only one of them, we kept all known

240   occurrences if the number of occupied grid cells in each country was >1 and

241   discarded singular casual occurrences at the country level. Although retaining

242   occurrences of taxa that were considered casual in a country meant

243   overestimation of the naturalized secondary range size in some cases, more

244   importantly, it allowed us to ameliorate the differences in expert judgment

245   regarding the degree of taxon establishment. Finally, we retained all native taxa

246   and non-native taxa that had established populations in Germany and the

247   Czech Republic in >1 grid cell across the study region. For consistency reasons,

248   we assigned a single, highest achieved degree of establishment to each taxon

249   (i.e., a taxon native in at least one country was treated as native across the study

250   area), which is in accordance with the national treatment of taxa having several

251   statuses in the country.

252   *Habitat affinity.* To enable analyses at the habitat level, we assigned each taxon

253   to at least one of the following six broad habitat types: forest, heathland and

254   scrub, grassland, wetland, rock and scree, and human-made. Information on

255   taxon habitat affinity was collated from multiple reference sources (namely,

11

256 BiolFlor, Kühn et al., 2004; Bundesamt für Naturschutz, 2017; EUNIS, Chytrý et

257 al., 2020; DAISIE, Roy et al., 2020; Divíšek et al., 2018; KORINA,

258 www.korina.info, accessed 4 August 2021; Sádlo et al., 2007), which used

259 different habitat classification schemes. We grouped the habitat types in each

260 data source into the six habitat types using expert knowledge (see Table S1 for

261 habitat classification) and then merged all the data. For taxa represented in

262 multiple sources, we only retained habitats listed in the majority of sources, to

263 avoid reports of sporadic occurrences.

264 *Traits.* We selected three traits for our analyses: (1) typical maximum plant

265 height (H_{max}; measured in m), (2) seed mass (*SM*; g), and (3) specific leaf area

266 (*SLA*; mm^2 mg^{-1}). These traits depict major plant life strategies (Díaz et al., 2016;

267 Westoby, 1998), correlate with many other important traits (Moles et al., 2007,

268 2009; Wright et al., 2004), act as both response and effect traits (Hanisch et al.,

269 2020; Kühn et al., 2021; Pollock et al., 2012), and are well represented in open

270 source trait databases (e.g., Kattge et al., 2020). We compiled trait data from

271 multiple databases and online resources: LEDA (Kleyer et al., 2008), TRY

272 (Kattge et al., 2011, 2020, accessed 1 October 2019; see Appendix S2 for

273 references within TRY), EcoFlora (Fitter & Peat, 1994, www.ecoflora.co.uk,

274 accessed 16 September 2021), Info Flora (www.infoflora.ch), iFlora (www.i-

275 flora.com), Kaplan et al., 2019, Vojtkó et al. (2020), World Species

276 (worldspecies.org). We included H_{max} measurements on vegetative and

277 generative organs, *SM* measurements on dried seeds, and *SLA* measurements on

278 sun and shade leaves and dry biomass. Where possible, we excluded trait

279 measurements from biomes outside our study area (e.g., tundra). Climbers were

280 excluded from analyses of H_{max}. In most cases, more than one trait value was

281 available per taxon. We used these values to calculate the geometric mean,

282 which is less sensitive to extreme values than other measures of central

283 tendency, after accounting for possible outliers; we calculated H_{max} as the

284 geometric mean of the maximum height values provided in each data source.

285 Additionally, we categorized each taxon as woody or herbaceous. Woody taxa

286 were defined as perennials whose stems were either entirely lignified or had a

287 lignified base. The information on woodiness was obtained directly or inferred

288 from life form and growth form using the following data sources: Zanne et al.,

289 2014 via the R package *growthform* (v.0.2.3; Taseski et al., 2019); LEDA (Kleyer

290 et al., 2008); BiolFlor (Kühn et al., 2004), Info Flora (www.infoflora.ch), Pladias

291 (www.pladias.cz); TRY (Kattge et al., 2011, 2020); Encyclopedia of Life

292 (eol.org). When the sources provided contrasting information, we assigned

293 woodiness based on morphological descriptions provided in floras. Woody

294 plants occurring in grasslands, wetlands, and rock and scree habitats were

295 excluded from all analyses. Due to the low sample size and variation in trait

296 values, we removed woody archaeophytes.

297 *Taxonomic names.* To facilitate name harmonization, we initially extracted all

298 the provided names including synonyms for each taxon in FloraWeb and

299 Pladias and matched taxa using those names. This resolved many cases that

300 would be problematic to standardize otherwise (e.g., a hybrid name in one

301 dataset and a corresponding hybrid formula in the other). Subsequently, we

302 checked and updated full taxonomic names against the Plants of the World

303 Online (POWO, 2022) using the R package *taxize* (Chamberlain & Szocs, 2013),

304 Leipzig Catalogue of Vascular Plants using the R package *lcvplants* (v.2.0;

305 Freiberg et al., 2020) and the GermanSL v1.5 checklist using the R package

306 *vegdata* (v.0.9.8; Jansen & Dengler, 2008, 2010). The use of multiple taxonomic

307 databases was necessary because our initial taxon list included many names

308 with qualifiers, hybrid formulas, aggregates, etc., for which none of the

309 available reference sources provided a single optimal solution. Taxonomically

310 critical taxa (e.g., those in genus *Taraxacum*, *Rubus*) were aggregated at higher

311 taxonomic levels (e.g., aggregate, section). Infraspecific taxa were generally

312 aggregated to species or higher levels unless they were non-native.

313   Our final dataset comprised 1,812 native, 181 archaeophyte, and 331

314 neophyte taxa; H_{max} was available for 96%, *SLA* for 74%, and *SM* for 88% of

315 those taxa.

316

Climate and land use data

318 *Baseline data.* We retrieved baseline data on 14 macroclimatic variables from

319 the 10' × 10' (*c.* 13 km × 18 km on the 50th parallel) CRU 1961–1990 dataset

320 (New et al., 2002). The variables were total annual precipitation (TAP; mm),

321 precipitation of the driest and wettest quarters (mm), precipitation of the driest

322 month (P_{dry}; mm), precipitation of the wettest month (P_{wet}; mm), precipitation

323 seasonality (coefficient of variation of monthly total precipitation, P_{CV}; %),

324 mean annual temperature (MAT; °C), mean and minimum temperature of the

325 coldest month (°C), mean temperature of the warmest month (°C), maximum

326 temperature of the warmest month (T_{warm}; °C), mean temperature of the driest

327 quarter (T_{dry}; °C), mean temperature of the wettest quarter (T_{wet}; °C), and

328 temperature seasonality (coefficient of variation of monthly average

329 temperature; %). These variables are commonly used in macroecological trait-

330 based studies (e.g., Boonman et al., 2020; Šímová et al., 2018; Wieczynski et al.,

331 2019) and have been projected under different climate scenarios (see below).

332 We rescaled all variables to the 10' × 6' spatial resolution by resampling original

333 values onto a 0.5' × 0.5' grid and then averaging obtained downscaled values

334 within each 10' × 6' grid cell using the R package *raster* (v.3.4-13; Hijmans,

335 2021). As a baseline for land use, we used Corine Land Cover (CLC) data for the

336 year 2000 (CLC, 2020), which we aggregated to the 10' × 6' spatial resolution

337 using the R package *raster* (Hijmans, 2021). Additionally, we determined which

338 of the six habitat types (see Habitat affinity) were present in each grid cell using

339 the Ecosystem types of Europe 2012 raster dataset (EEA, 2018). Forests,

340 grasslands, and human-made habitats were present in all 3,031 grid cells,

341 whereas heaths and scrub occurred in 2,091, wetlands in 966, and rock and

342 scree habitats in 337 grid cells.

343 *Scenario projections.* We obtained climate and land-use projections for the

344 period of 2081–2100 from the IMPRESSIONS project (www.impressions-

345 project.eu). The core of the project is the IMPRESSIONS Integrated Assessment

346 Platform (IAP2), which combines a suite of sectoral models within a web-based

347   platform and generates quantitative future projections for multiple indicators

348   across Europe at 10' × 10' spatial resolution. The IAP2 includes three

349   Representative Concentration Pathways (RCP2.6, RCP4.5, and RCP8.5) and

350   four European Shared Socio-Economic Pathways (Eur-SSP1, Eur-SSP3, Eur-

351   SSP4, and Eur-SSP5; Kok et al., 2019) and permits modeling individual and

352   joint impacts of climate and socio-economic change until 2100. As part of its

353   output, the IAP2 provides per-cell area proportions of seven land-use types

354   (arable, intensive grassland, extensive grassland, urban, managed forest,

355   unmanaged woodland, and unmanaged land). We downloaded climate

356   projections directly from the IMPRESSIONS data repository

357   (ensemblesrt3.dmi.dk/data/IMPRESSIONS; accessed 10 August 2020). To

358   simulate land use projections, we ran the IAP2 for baseline conditions and for 7

359   combinations of climate and socio-economic scenarios, for each using 3

360   different dynamically downscaled CMIP5 climate models (listed in Table S2).

361   Next, we matched land use classes in CLC and IAP2 and evaluated the

362   agreement at the 10' × 10' resolution between the two baseline datasets. The

363   agreement was high only for urban land, whereas other land-use types showed

364   considerable disagreement (Pearson's r = 0.15–0.68), based on which we used

365   only the percentage of urban land ($U_\%$) in further analyses. We did not consider

366   using the baseline IAP2 projections to parametrize our models because of their

367   inferior spatial resolution and accuracy compared to CLC data.

368

369   2.3 Data analyses

Data preparation

370

371   We first log$_{10}$-transformed all traits to reduce the skewness of their

372   distributions and the effect of extreme values. Then, separately for woody and

373   herbaceous native, neophyte, and archaeophyte taxa within selected habitats,

374   we averaged each trait at the grid cell level, omitting taxa with missing trait

375   values. This means that when all the 6 habitat types were present in a grid cell,

376   we computed up to 24 mean values per trait per grid cell (after excluding

377   woody archaeophytes across all habitats and all woody taxa in grasslands,

378   wetland, and rock and scree; see above). The obtained trait mean values were

379   used as response variables in statistical models. Trait means based on less than 4

380   taxa were heuristically excluded from analyses. For analyses, we separately

381   scaled trait means of woody and herbaceous native, neophyte, and

382   archaeophyte plant assemblages at the habitat level to zero mean and unit

383   variance. We did so because we aimed to capture how taxon status, woodiness,

384   and habitat moderated the effects of climate and land use, rather than to

385   quantify their direct effects on traits. Moreover, such scaling allowed us to

386   impose a single spatial autocorrelation structure across habitats and thus

387   quantify all effects within a single model (as opposed to, for example, fitting a

388   separate model for each habitat type).

389   To reduce the redundancy among the potential environmental predictor

390   variables, we performed variable selection based on the variance inflation factor

391   (VIF) and Pearson's correlation coefficient (r) using the functions *'vifstep'* and

392   *'vifcor'*, respectively, in the R package *usdm* (v.1.1-18; Naimi et al., 2014). Out

393 of the initial 15 predictor variables, we retained 8 (7 variables with VIF <10 and

394 one additional with $|r| <0.7$). Namely, we kept P_{dry}, P_{wet}, P_{CV}, T_{cold}, T_{warm}, T_{dry},

395 $T_{wet,}$ and $U_{\%}$. Prior to analyses, we scaled these variables to the mean of zero and

396 unit variance to aid model parametrization and interpretation. The per-cell

397 number of taxa (N_{taxa}), which we controlled for in analyses, was scaled similarly

398 to trait values.

399

Statistical models

401 We assessed trait– environment relationships using linear multilevel models.

402 All models were parameterized within the full Bayesian framework using the

403 Hamiltonian Monte Carlo sampling algorithm implemented in the modeling

404 software Stan (Carpenter et al., 2017) via the function '*brm*' in the R package

405 *brms* (v.2.14.4; Bürkner, 2017). We modeled individual trait per-cell mean

406 values as the function of climatic variables and $U_{\%}$ (continuous predictors) and

407 taxon biogeographical status, woodiness, and habitat (categorical predictors).

408 More specifically, we developed a suite of slope-only models, in which we

409 included a single continuous predictor and its two- and three-way interactions

410 with taxon status and woodiness that were allowed to vary by habitat (i.e.,

411 habitat was modeled as a group-level effect). We excluded the main effects of

412 origin, woodiness, and habitat from the models, as those equaled 0 due to the

413 prior scaling of response variables (see Data preparation). The models allowed

414 us (1) to quantify the extent to which the effects of climate and the level of

415 urbanization differ across native and non-native taxa, herbaceous and woody

416 taxa, as well as different habitats, and (2) to incorporate this potential context-

417 dependency into future projections of spatial trait distributions. To account for

418 residual spatial autocorrelation, we included conditional autocorrelation

419 structure (CAR) with grid cell identifier as a grouping factor in all our models.

420 Additionally, in all our models we controlled for N_{spp}, by including this metric

421 as another predictor variable because sometimes average trait values were

422 correlated with N_{spp}. In particular, this correlation was negative for H_{max},

423 suggesting that taxon-richer grid cells had on average a higher proportion of

424 shorter taxa. Such a pattern may reflect sampling effort (e.g., smaller plants are

425 more likely to remain undetected; Chen et al., 2013) as well as present a

426 genuine ecological phenomenon (Aarssen et al., 2006). In either case, we chose

427 to control for N_{taxa} in our models, as otherwise its effect could be incorrectly

428 attributed to the environmental predictors. A model for each environmental

429 predictor can be written as follows:

$$y_i \sim \beta_{j[i]}^{ew} e_i w_i + \beta_{j[i]}^{es} e_i s_i + \beta_{j[i]}^{ews} e_i w_i s_i + \beta_{j[i]}^{nws} n_i w_i s_i + \epsilon_i + z_{k[i]}$$

$$\beta_j^{ew} \sim N(\mu_{ew}, \sigma_{ew}^2)$$

$$\beta_j^{es} \sim N(\mu_{es}, \sigma_{es}^2)$$

$$\beta_j^{ews} \sim N(\mu_{ews}, \sigma_{ews}^2)$$

$$\beta_j^{nws} \sim N(\mu_{nws}, \sigma_{nws}^2)$$

$$\epsilon \sim N(0, \sigma_y^2)$$

$$z_k \sim N(0, \Sigma)$$

430 where y_i is the per-cell mean trait value for the ith observation ($i = 1, \ldots, N_{\text{obs}}$),

431 calculated for each combination of habitat type, woodiness and biogeographical

432 status; e_i is the environmental predictor; w_i is woodiness; s_i is biogeographical

433 status; n_i is the number of taxa; β_j^{ew}, β_j^{es}, β_j^{ews}, β_j^{nws} are slopes for the

434 interactions between variables indicated in the superscript in the jth habitat type

435 ($j = 1, \ldots, N_{\text{habitats}}$); β_j^{es} is the slope for the interaction between e_i and s_i in the jth

436 habitat type; β_j^{ews} is the slope for the interaction between e_i, w_i and s_i in the jth

437 habitat type; ϵ_i is the residual effect of the ith observation; z_k is the residual

438 spatial random error for the kth grid cell ($k = 1, \ldots, N_{\text{cells}}$); μ_{ew}, μ_{es}, μ_{ews}, μ_{ews}

439 are the overall slopes for the interactions specified in the subscript; σ_{ew}^2, σ_{es}^2,

440 σ_{ews}^2, σ_{nws}^2 are the habitat-level variances for the slopes; σ_y^2 is the residual

441 variance; and Σ is the covariance matrix, as defined in a conditional

442 autoregressive model. We chose to fit separate models for each environmental

443 predictor because of the high complexity of a full model (i.e., for each

444 environmental predictor, we estimated 12 model parameters) and possible

445 collinearity due to a large number of interaction terms with the same

446 categorical predictors.

447   To prevent the sampler from considering highly implausible values, we

448 used zero-centered weakly informative priors, which we chose based on prior

449 predictive checks (Wesner & Pomeranz, 2021). For each model, we ran 4 chains

450 with 10,000 iterations per chain, starting from default values. We discarded the

451 first half of each chain as a warm-up and thinned the other half at the interval

452 of 4, which resulted in 5000 draws from the posterior distribution for each

453   parameter. The potential scale reduction factor, $\hat{R}$ (Gelman & Rubin, 1992), was

454   close to 1 for all our models, indicating convergence.

455

Model predictive performance

457   We evaluated model predictive performance using exact k-fold cross-validation.

458   To avoid the potential overestimation of predictive performance, the folds were

459   determined as spatial blocks (Roberts et al., 2017). For that, we overlaid a 3×3

460   spatial-block grid onto the grid of the study area (Figure S1) using the function

461   *'spatialBlock'* in the R package *blockCV* (v2.1.4; Valavi et al., 2019), which

462   resulted in 8 spatial blocks, two of which we subsequently merged to achieve a

463   more even distribution of grid cells across folds. We then assigned all data

464   points within a grid cell to a specific fold and performed a 7-fold cross-

465   validation with the function *'kfold'* in the R package *brms* (Bürkner, 2017). As

466   the measures of model predictive performance, we calculated the k-fold

467   information criterion (*kfoldIC*) and the root mean square error based on cross-

468   validated predictions (*RSME*; Table S3).

469

Future projections

471   For each trait, we obtained projections of per-cell mean trait values on baseline

472   and scenario data (7 RCP–SSP scenario combinations $\times$ 3 dynamically

473   downscaled CMIP5 climate models for each RCP; see Table S1). We set the

474   scaled N_{taxa} to 0 in all projections. These projections were computed as the

475   weighted average of posterior predictive distributions from the eight models

476   each with a single environmental predictor variable. For averaging, we used

477   Bayesian stacking of predictive distributions (Yao et al., 2018), a method that

478   explicitly optimizes individual model weights to maximize the leave-one-out

479   predictive density. As input for Bayesian stacking, we provided the expected log

480   pointwise predictive densities based on the results of k-fold cross-validation.

481   We then calculated the projected per-cell change in each trait under each

482   scenario as the difference between the medians of the projected future and

483   baseline posterior predictive distributions. To enable comparison across

484   biogeographic statuses, we rescaled trait change values of archaeophytes and

485   neophytes to the standard deviations (SD) of a baseline trait distribution for

486   native taxa of corresponding woodiness and habitat. To assess the overall

487   magnitude of trait change, we calculated a Euclidean distance between

488   projected per-cell posterior means of the three traits on the baseline data and

489   scenario data.

490   To summarize the effects of all environmental predictors across all three

491   traits and to visualize the direction of those effects in the multivariate space, we

492   performed separate redundancy analyses (RDA) on the subsets of the projected

493   trait change that corresponded to all unique combinations of biogeographical

494   status, woodiness, and habitat across all the scenarios using the R package *vegan*

495   (v.2.5-7; Oksanen et al., 2020). As the measure of individual predictor

496   contribution, we calculated the length of the vectors with the initial point at

497   (0,0) and the terminal point at the scores of the first two RDA axes. The vectors

498   reflected the weighted effect sizes of the predictors that were used to calculate

499   posterior predictive distributions.

500   All statistical analyses and visualizations were performed in the R

501   environment v4.1.0 (R Core Team, 2021).

502

503   **3 RESULTS**

504   Overall, we observed a high degree of variability (i.e., the spread across

505   posterior distributions) and uncertainty (i.e., the spread within posterior

506   distributions) in the magnitude and direction of the projected per-cell change

507   in maximum height (H_{max}), specific leaf area (*SLA*), and seed mass (*SM*) under

508   environmental change scenarios. The variation in the projected trait change

509   was pronounced at all three grouping levels considered in the analyses, i.e.,

510   taxon biogeographical status, woodiness, and habitat type, and increased with

511   the degree of environmental change (Figures 1–4, S2–S7, S14). Likewise, the

512   degree of uncertainty associated with individual per-cell projections varied

513   across the grouping levels and was generally higher under more extreme

514   scenarios, being driven much more by climate change than urbanization

515   (Figures S8–S13). The lowest likelihood of trait change (i.e., >50% grid cells

516   with projected posterior credible intervals excluding zero) was observed under

517   RCP4.5 and RCP8.5 for woody native *SLA* in human-made habitats and for

518   archaeophyte *SM* in human-made habitats and heaths and scrub.

519   Below, we focus on the posterior means of the projected per-cell

520   posterior distributions, which reflect the overall trends in our projections but

521   do not embrace the uncertainty, for the least and most extreme scenarios

522   (RCP2.6 Eur-SSP1 and RCP8.5 Eur-SSP5, respectively) to illustrate the

523   maximum future option space for 2081–2100. The results for other scenarios are

524   presented in the Supplementary Material.

525

3.1 Projected trait change

527   When all traits were considered, the magnitude of trait change was expected to

528   be on average higher in forests, heaths and scrub, and grasslands than in other

529   habitat types (Figure 1a), for non-natives than natives (Figure 1b), and for

530   woody than herbaceous plants (Figure 1c). The direction of the projected

531   individual trait change often diverged for herbaceous vs. woody plants as well

532   as for natives vs. neophytes (Figure S14).

533   In all scenarios, the mean trend for H_{max} of herbaceous plant assemblages

534   in tree- and shrub-dominated habitats was positive throughout the study area,

535   being more pronounced for archaeophytes and neophytes than for natives

536   (Figures 2a,c, S2a–f). In other habitats, the change of H_{max} was expected to be

537   more heterogeneous spatially and across biogeographical statuses. Notably, in

538   grassland and rock and scree habitats, herbaceous native H_{max} was projected to

539   show very little to no change, whereas herbaceous neophytes were anticipated

540   to increase in H_{max}, especially in grasslands (Figure 2a,c, S2g–l, S15a,c). As for

541   woody plant assemblages, only H_{max} of natives demonstrated a predominantly

542   positive trend, with the highest increase projected for human-made habitats

543   under RCP8.5 SSP5; meanwhile, H_{max} of neophytes tended to mostly decrease

544   (Figures 2b,d, S3, S15b,d).

545   Similar to H_{max}, the projected change of *SLA* varied with taxon

546   biogeographical status, woodiness, and habitat (Figures 3, S4–5). Herbaceous

547   *SLA* was projected to mainly decrease, with some exceptions (e.g., native *SLA*

548   in wetlands; Figures 3a,c, S4). At the same time, the degree of this decrease

549   tended to be lower for natives than neophytes (S16a,c). In contrast, woody *SLA*

550   was anticipated to increase for both natives and neophytes, with the latter

551   increasing more than natives in forest and heaths and scrub habitats (Figures

552   3b,d, S5, S16b,d).

553   The overall magnitude of *SM* change was comparable to that of H_{max} and

554   *SLA*. In forests and heaths and scrub, woody native and non-native *SM* was

555   projected to only increase, whereas in human-made habitats neophyte *SM*

556   showed a decline (Figures 4b,d, S7a–e, S17b,d). The direction of projected

557   change in herbaceous *SM* was less uniform and varied spatially and with habitat

558   and biogeographical status (Figures 4a,c, S6, S17a,c). Particularly, *SM* of

559   archaeophytes tended to respond opposingly to natives and neophytes and was

560   more likely to decrease in the majority of habitats (Figures 4a,c, S6).

561

562   ### 3.2 Contribution of environmental predictors

563   Across all three traits, T_{warm} and T_{cold} captured the highest amount of variation

564   in the projected trait change, followed by P_{CV}, P_{dry}, and P_{wet}; the contributions

565   of T_{dry}, T_{wet}, and $U_{\%}$ were considerably smaller (Figure S18). The role of

566   individual environmental predictors generally varied with taxon

567   biogeographical status, habitat, and woodiness (Figure 5). Nonetheless, some

568   predictors showed highly consistent associations with the projected trait

569   change. For example, a projected increase in herbaceous SM correlated mostly

570   positively with P_{CV} and negatively with P_{dry}; the opposite was, however,

571   observed for herbaceous neophyte SM in forest, heaths and scrub, and rock and

572   scree habitats. Similarly, T_{cold} contributed positively to the SM increase in

573   woody plant assemblages, apart from neophytes in human-made habitats.

574   Meanwhile, T_{warm} and T_{cold} exhibited a strong positive relationship with both

575   herbaceous and woody H_{max}, except for human-made habitats and woody

576   neophytes, for which the relationship was reverse. In some cases, the effect of

577   temperature on H_{max} was not as pronounced as that of P_{wet} and P_{CV}. Particularly,

578   native H_{max} in grasslands and human-made habitats was strongly positively

579   affected by P_{wet} and P_{CV}, whereas in rock and scree habitats native H_{max} was

580   negatively associated with the two predictors. With few exceptions, herbaceous

581   SLA correlated negatively with T_{warm}, T_{cold}, and P_{dry}. Additionally, native

582   herbaceous SLA positively correlated with P_{wet} in all habitats apart from

583   wetlands, whereas non-native herbaceous SLA consistently showed a negative

584   relationship with P_{wet}. Unlike herbaceous SLA, native and neophyte woody SLA

585   was strongly positively related to T_{warm}, T_{cold}, and P_{dry} (Figure 5).

586

4 DISCUSSION

588   In this study, we quantified the broad-scale relationships of three traits central

589   to plant life history – maximum plant height (H_{max}), specific leaf area (SLA), and

590   seed mass (SM) – with eight selected environmental variables, and used the

591   obtained relationships to project the trait change under seven plausible

592   scenarios of future environmental change in Central Europe. We explicitly

593   modeled the variation in trait–environment relationships associated with plant

594   woodiness, biogeographical status, and habitat type, to account for the fact that

595   different types of plant assemblages may exhibit unique adaptations to the

596   environment, hence making some aspects of mechanistic context-dependence

597   explicit (Catford et al., 2021). We showed that the three traits were projected

598   both to increase and decrease to varying degrees across and – in many cases –

599   within habitats and that the overall magnitude of this change was expected to

600   be on average higher for non-native than native taxa (Figure 1b) and under

601   more extreme scenarios (Figures S2–S7). Moreover, we found that in the future,

602   distinct environmental responses of native and non-native plants may lead to

603   even higher trait values than currently observed for non-natives (e.g.,

604   herbaceous H_{max} in most habitats) as well as to a reduced average native–non-

605   native trait difference (e.g., woody H_{max}; Figures S15–17), which may result in

606   altered competitive hierarchies among natives and non-natives (Kunstler et al.,

607   2016).

608

4.1 Projected overall trait change across habitat types

609

610 The overall magnitude of trait change was projected to be higher in forests,

611 heaths and scrub, and grassland habitats compared to rock and scree, wetland,

612 and human-made habitats (Figure 1a). This result, at least for wetlands and rock

613 and scree habitats, may reflect both the low sensitivity of these habitat types to

614 the environmental change as well as the limitations of our approach to capture

615 environmentally-driven trait variation at smaller scales. In particular, rock and

616 scree habitats are highly stable systems defined by environmental stress more

617 than by macroclimate, whereas wetlands are strongly shaped by local

618 hydrology, which we did not account for, and show much less turnover along

619 macroclimatic gradients than other habitats. Moreover, the spatial resolution of

620 our analyses might have been too coarse to capture the environmental gradients

621 that traits of wetland and rock and scree plant assemblages respond to. Human-

622 made habitats, on the other hand, are typically more environmentally

623 homogeneous and generally contain plants that are pre-adapted to disturbance

624 and warm and dry conditions (Kalusová et al., 2017). Therefore, it is expected

625 that human-made habitats would often contain plant taxa characterized by

626 relatively large *SLA* and small *SM*, irrespective of macroclimate. Nevertheless,

627 this result once again underlines the importance of incorporating habitat

628 information into macroecological analyses, as failing to do so might blur the

629 environmental signals that exist at a particular spatial scale.

630

4.2 Projected change in maximum height

631

632　Our results showed that the hierarchy of environmental drivers shaping the

633　large-scale distribution of plant height is largely habitat-specific and that the

634　trait patterns found across non-native plant assemblages often deviate from

635　those found in native assemblages. Specifically, temperature plays the dominant

636　role in the projected change of H_{max} in forests and heaths and scrub, while in

637　other habitats, the effect of precipitation prevails. Similarly, a strong positive

638　association between temperature and plant height has been detected across

639　habitat types and within specific habitats at the continental (e.g. Šímová et al.,

640　2018; forest understories, Padullés Cubino et al., 2021) and regional scales (e.g.,

641　forest understories, Maes et al., 2020; mountain grasslands and rock and scree,

642　Dubuis et al., 2013). Moles et al. (2009), on the other hand, reported that the

643　best predictor of plant height at the global scale is the precipitation of the

644　wettest month, which is supported by our results for H_{max} in grasslands and

645　rock and scree habitats. Interestingly, while the relationships for native woody

646　assemblages add to the current consensus on the effect of climate on woody

647　plant height (Šímová et al., 2018; Swenson et al., 2012), the results for

648　neophytes may suggest that woody non-natives are preadapted to a different

649　subgradient of the global climatic gradient – in particular, to hotter and drier

650　conditions – where the opposite, negative relationship with temperature can

651　occur (Madani et al., 2018; Moles, 2018). A negative relationship between H_{max}

652　of invasive neophytes and T_{cold} was also shown by Milanović et al. (2020),

653　although the mechanisms behind this phenomenon remain unclear.

654

4.3 Projected change in specific leaf area

655

656   Contrary to several previous studies (Dubuis et al., 2013; Rosbakh et al., 2015;

657   Šímová et al., 2018), herbaceous native and neophyte SLA correlated primarily

658   negatively with temperature, and only herbaceous archaeophyte SLA tended to

659   show the opposite. Somewhat unexpectedly, another pronounced driver of

660   herbaceous SLA change, P_{dry}, also had mainly a negative effect on SLA across all

661   herbaceous assemblages, whereas P_{wet} had a positive and negative influence on

662   herbaceous native and neophyte SLA, respectively (Figure 5). A negative shift

663   of native SLA along the P_{dry} gradient appears in disagreement with a previously

664   documented negative effect of drought on SLA (Wellstein et al., 2017; Wright

665   et al., 2005). This pattern may be attributed to the fact that within Central

666   Europe, plants with evergreen, low-SLA leaves predominantly occur in the

667   mountains (where precipitation is high) (Chytrý et al., 2021). In contrast to

668   herbaceous SLA yet in alignment with previous reports (Šímová et al., 2018;

669   Swenson et al., 2012), SLA across all woody assemblages exhibited a strong

670   positive relationship with temperature as well as P_{dry}. As a result, it is predicted

671   that environmental change will lead to an increase in woody native SLA and

672   even more so in woody neophyte SLA (Figures 3b,d, 5, S5), which may allow

673   non-natives to gain a further advantage over natives (Pyšek & Richardson,

674   2008).

675   Reflecting the combined effect of all the predictors, our projections

676   forecasted mostly a decrease in herbaceous SLA; an increase throughout the

677   study area was projected only for native herbaceous SLA in wetlands and

678 archaeophyte *SLA* in forests, and a partial increase in *SLA* was projected for
679 archaeophytes in wetlands and human-made habitats and for herbaceous
680 neophytes in grasslands and human-made habitats (Figures 3, S4). Despite a
681 general projected shift towards more conservative resource-use strategies, our
682 projections suggest that herbaceous neophyte *SLA* will be affected less than that
683 of herbaceous natives (Figures S4, S16). This may lead to a further increase in
684 the *SLA* imbalance between native and non-native taxa towards the latter in
685 the region (Divíšek et al., 2018), possibly resulting in an even higher proportion
686 of invasive non-natives (Pyšek & Richardson, 2008). The alteration of the *SLA*
687 composition will undoubtedly affect ecosystem functioning. For example, an
688 overall decrease of *SLA* in grasslands may lead to higher root biomass
689 (Klimešová et al., 2021) and total soil carbon (Garnier et al., 2004), as well as
690 reduced nutrient cycling (Lavorel et al., 2011) and productivity (Brun et al.,
691 2022).

692

693 ## 4.4 Projected change in seed mass

694 Our results show that overall drier, less stable climates may on average
695 contribute to an increase in herbaceous *SM* but a decrease in woody *SM*. This
696 finding is congruent with previous studies (Baker, 1972; Dubuis et al., 2013;
697 Šímová et al., 2015; Swenson et al., 2012; Vandelook et al., 2018) and at least
698 partially explains the heterogeneous relationships of *SM* and precipitation in
699 the literature (discussed in Moles, 2018). Notably, while this pattern holds for
700 natives and archaeophytes across all habitats, neophytes often deviate from it.

701   Specifically, we observed the opposite effect of the precipitation amount and

702   seasonality on herbaceous neophyte SM in tree- and shrub-dominated as well as

703   rock and scree habitats and on woody neophyte SM in human-made habitats

704   (Figures 5, S14). Such divergence from native herbaceous SM may be

705   confounded with the turnover in the growth form, i.e., the proportional

706   increase of small-seeded, short-leaved neophytes in drier areas (Sandel et al.,

707   2010). Additionally, the contrasting responses of native and non-native plant

708   assemblages to precipitation may be due to the differences in the duration of

709   their exposure to the environment and the fact that many non-natives are still

710   actively spreading. For archaeophytes, the positive effect of precipitation is

711   likely to be overwhelmed by the negative effect of higher temperatures, leading

712   to the overall decrease in SM (Figures 4, S6). Importantly, for woody SM, the

713   overall effect of precipitation may be not as pronounced as that of temperature.

714   Particularly, our results point to a strong positive association of woody SM with

715   T_{warm} and T_{cold} (Figure 5), which drives the projected increase in woody SM

716   (Figures 4b,d, S7). This is in line with previous studies, which also documented

717   a strong positive effect of temperature on SM of woody plants (Moles et al.,

718   2014; Šímová et al., 2015, 2018; Swenson et al., 2012) and highlighted that

719   herbaceous SM is less sensitive to temperature than woody SM (Šímová et al.,

720   2018).

721

722   4.5 Differences in the response between native and non-native taxa

723 The observed differences between native and non-native plant assemblages

724 once again point out that biogeographical origin affects species performance, via

725 eco-evolutionary novelty of non-natives (Heger et al., 2019; Saul et al., 2013) or

726 due to their pre-adaptation to specific conditions (Maron et al., 2004). For

727 example, non-native species often originate from more nitrogen-rich habitats

728 (Dostál et al., 2013) and therefore are characterized by higher *SLA*. In the long

729 run, the differential response of native and non-native species to environmental

730 factors might lead to even stringer differences in their trait compositions, and

731 this is especially likely for neophytes. Such differences suggest that ecosystem

732 functions provided by future neophyte assemblages may not be redundant to

733 those currently provided by natives. On the contrary, functions currently

734 provided by natives may be replaced with different functions provided by

735 neophytes, thus leading to the increase of functional turnover rather than its

736 buffering in the course of global change.

737

738 ### 4.6 Study shortcomings

739 In our analyses, we aggregated plant trait data to the taxon level and then to the

740 10' × 6' grid-cell level for a total of 24 unique assemblages defined by plant

741 woodiness, biogeographical status, and habitat type. Although this precluded us

742 from incorporating intraspecific trait variation, the resolution of trait data was

743 sufficient to accurately model the trait variation due to species sorting as the

744 function of environmental predictors. Moreover, we ensured that trait data

745 were representative of our study area by primarily using data sources for

746   Central Europe and where possible excluding data from environments not

747   found in Germany or the Czech Republic. Additionally, the decisions made

748   during data preparation (e.g., the use of geometric vs. arithmetic mean for trait

749   averaging) might have to a certain extent influenced our results, especially for

750   non-native plants, whose number per grid cell was typically low. This problem,

751   however, was to some extent ameliorated by partial pooling of parameter

752   estimates for different plant assemblages within the multilevel modeling

753   framework. We generated trait change projections using Bayesian stacking of

754   predictive distributions from individual-predictor models (Yao et al., 2018),

755   instead of parametrizing predictive models with all environmental predictors at

756   once. In our case, the latter was difficult to implement because the same

757   categorical variables (i.e., woodiness and biogeographical status) would be

758   included in many interaction terms with intercorrelated environmental

759   predictors (Figure S19), which might have led to spurious results (Duncan &

760   Kefford, 2021). Finally, the obtained projections of future trait change were

761   highly uncertain (Figures S8–13), which indicates that other important

762   predictors of trait composition need to be identified and incorporated into

763   further analyses (e.g., soil variables, Joswig et al., 2022).

764

765   ## 4.7 Conclusions

766   In this study, we assessed how habitat-specific plant trait values might shift

767   under future environmental change. Our results depicted the frequently

768   neglected distinctions in trait–environment relationships that are contingent

769   upon plant woodiness, biogeographical status, and habitat type, thereby

770   explaining some of the existing idiosyncrasies within the literature and

771   producing more informative and refined projections of future trait changes. The

772   obtained projections, although uncertain and requiring more global change

773   drivers to factor in, provide an insightful perspective on the conditions under

774   which non-native plants may prevail over natives and vice versa and can serve

775   as a starting point for exploring changes in ecosystem functions and services in

776   a rapidly changing world.

777

ACKNOWLEDGEMENTS

791

792   CONFLICT OF INTEREST

793   The authors declare that there is no conflict of interest.

794

795   AUTHOR CONTRIBUTIONS

796   IK and SK conceived the initial idea of the study, which was further developed

797   by MG. MG collected the data, performed statistical analyses, and wrote the

798   first draft of the manuscript. All authors contributed critically to the drafts and

799   gave final approval for publication.

800

801   DATA AVAILABILITY STATEMENT

802   All data used in this study are freely available online.

803

804   ORCID

805   Marina Golivets https://orcid.org/0000-0003-1278-2663

806   Ingolf Kühn https://orcid.org/0000-0003-1691-8249

807   Sonja Knapp https://orcid.org/0000-0001-5792-4691

808   Bernd Lenzner https://orcid.org/0000-0002-2616-3479

809   Guillaume Latombe https://orcid.org/0000-0002-8589-8387

810   Franz Essl https://orcid.org/0000-0001-8253-2112

811   Brian Leung https://orcid.org/0000-0002-8323-9628

812

813   REFERENCES

814   Aarssen, L. W., Schamp, B. S., & Pither, J. (2006). Why are there so many small plants? Implications for species
815   coexistence. *Journal of Ecology*, *94*(3), 569–580.

816 Axmanová, I., Kalusová, V., Danihelka, J., Dengler, J., Pergl, J., Pyšek, P., Večeřa, M., Attorre, F., Biurrun, I., &
817   Boch, S. (2021). Neophyte invasions in European grasslands. *Journal of Vegetation Science*, *32*(2),
818   e12994.
819 Baker, H. G. (1972). Seed weight in relation to environmental conditions in California. *Ecology, 53*(6), 997–
820   1010.
821 Beals, E. W. (1984). Bray-Curtis ordination: An effective strategy for analysis of multivariate ecological data.
822   *Advances in Ecological Research*, *14*, 1–55.
823 Bjorkman, A. D., Myers-Smith, I. H., Elmendorf, S. C., Normand, S., Rüger, N., Beck, P. S., Blach-Overgaard,
824   A., Blok, D., Cornelissen, J. H. C., & Forbes, B. C. (2018). Plant functional trait change across a
825   warming tundra biome. *Nature*, *562*(7725), 57–62.
826 Boonman, C. C., Benítez-López, A., Schipper, A. M., Thuiller, W., Anand, M., Cerabolini, B. E., Cornelissen, J.
827   H., Gonzalez-Melo, A., Hattingh, W. N., & Higuchi, P. (2020). Assessing the reliability of predicted
828   plant trait distributions at the global scale. *Global Ecology and Biogeography*, *29*(6), 1034–1051.
829 Bundesamt für Naturschutz. (2017). *Bewertungsschemata für die Bewertung des Erhaltungsgrades von Arten*
830   *und Lebensraumtypen als Grundlage für ein bundesweites FFH-Monitoring. Teil II: Lebensraumtypen*
831   *nach Anhang I der FFH-Richtlinie (mit Ausnahme der marinen und Küstenlebensräume). BfN-*
832   *Skripten 481.* Bonn, Germany.
833 Bürkner, P.-C. (2017). brms: An R package for Bayesian multilevel models using Stan. *Journal of Statistical*
834   *Software*, *80*(1), 1–28.
835 Carmona, C. P., & Pärtel, M. (2021). Estimating probabilistic site-specific species pools and dark diversity from
836   co-occurrence data. *Global Ecology and Biogeography*, *30*(1), 316–326.
837 Carpenter, B., Gelman, A., Hoffman, M. D., Lee, D., Goodrich, B., Betancourt, M., Brubaker, M., Guo, J., Li, P.,
838   & Riddell, A. (2017). Stan: A probabilistic programming language. *Journal of Statistical Software*, *76*(1),
839   1–32.
840 Catford, J. A., Wilson, J. R., Pyšek, P., Hulme, P. E., & Duncan, R. P. (2021). Addressing context dependence in
841   ecology. *Trends in Ecology & Evolution 37*(2): 158–170.
842 Český hydrometeorologický ústav. (2019). *Aktualizace Komplexní studie dopadů, zranitelnosti a zdrojů rizik*
843   *souvisejících se změnou klimatu v ČR z roku 2015.* 384 pages.
844 Chamberlain, S., & Szocs, E. (2013). taxize - taxonomic search and retrieval in R. *F1000Research, 2*(191).
845 Chen, G., Kéry, M., Plattner, M., Ma, K., & Gardner, B. (2013). Imperfect detection is the rule rather than the
846   exception in plant distribution studies. *Journal of Ecology, 101*(1), 183–191.
847 Chytrý, M., Danihelka, J., Kaplan, Z., Wild, J., Holubova, D., Novotný, P., ... & Pyšek, P. (2021). Pladias
848   Database of the Czech flora and vegetation. *Preslia 93*(1): 1–87.
849 Chytrỳ, M., Tichỳ, L., Hennekens, S. M., Knollová, I., Janssen, J. A., Rodwell, J. S., Peterka, T., Marcenò, C.,
850   Landucci, F., & Danihelka, J. (2020). EUNIS Habitat Classification: Expert system, characteristic species
851   combinations and distribution maps of European habitats. *Applied Vegetation Science*, *23*(4), 648–675.
852 CLC. (2020). *Corine Land Cover. Version 2020 20u1.* Available from: https://land.copernicus.eu/pan-
853   european/corine-land-cover/clc-2000
854 Daru, B. H., Davies, T. J., Willis, C. G., Meineke, E. K., Ronk, A., Zobel, M., ... & Davis, C. C. (2021).
855   Widespread homogenization of plant communities in the Anthropocene. *Nature communications,*
856   *12*(1), 1–10.

857 Datenbank FlorKart, BfN und NetPhyD. (2013). *Datenbank FlorKart der Floristischen Kartierung Deutschlands,*
858   *Stand 2013, Bundesamt für Naturschutz (BfN) und Netzwerk Phytodiversitaet Deutschland (NetPhyD).*

859 Díaz, S., Kattge, J., Cornelissen, J. H., Wright, I. J., Lavorel, S., Dray, S., Reu, B., Kleyer, M., Wirth, C., &
860   Prentice, I. C. (2016). The global spectrum of plant form and function. *Nature*, *529*(7585), 167–171.

861 Díaz, S., Settele, J., Brondízio, E. S., Ngo, H. T., Agard, J., Arneth, A., Balvanera, P., Brauman, K. A., Butchart, S.
862   H., & Chan, K. M. (2019). Pervasive human-driven decline of life on Earth points to the need for
863   transformative change. *Science*, *366*(6471), eaax3100.

864 Divíšek, J., Chytrý, M., Beckage, B., Gotelli, N. J., Lososová, Z., Pyšek, P., Richardson, D. M., & Molofsky, J.
865   (2018). Similarity of introduced plant species to native ones facilitates naturalization, but differences
866   enhance invasion success. *Nature Communications*, *9*(1), 1–10.

867 Dostál P., Dawson W., van Kleunen M., Keser L. H., & Fischer M. (2013). Central European plant species from
868   more productive habitats are more invasive at a global scale. *Global Ecology and Biogeography, 22*, 64–
869   72.

870 Drenovsky, R. E., Grewell, B. J., D'antonio, C. M., Funk, J. L., James, J. J., Molinari, N., Parker, I. M., &
871   Richards, C. L. (2012). A functional trait perspective on plant invasion. *Annals of Botany*, *110*(1), 141–
872   153.

873 Dubuis, A., Rossier, L., Pottier, J., Pellissier, L., Vittoz, P., & Guisan, A. (2013). Predicting current and future
874   spatial community patterns of plant functional traits. *Ecography*, *36*(11), 1158–1168.

875 Duncan, R. P., & Kefford, B. J. (2021). Interactions in statistical models: Three things to know. *Methods in*
876   *Ecology and Evolution, 12*(12), 2287-2297.

877 DWD. (2018). *Climate predictions and climate projections.* Deutscher Wetterdienst, Offenbach am Main,
878   Germany, 28 pages.

879 DWD. (2017). Climate Data Center. Available at: ftp://ftp-cdc.dwd.de/pub/CDC.

880 EEA. (2021). Land cover country fact sheets 2000-2018. https://www.eea.europa.eu/themes/landuse/land-cover-
881   country-fact-sheets [accessed July 19, 2021].

882 EEA. (2018). Ecosystem types of Europe 2012 - Terrestrial habitats reliability map, version 3.1.

883 Eichenberg, D., Bowler, D. E., Bonn, A., Bruelheide, H., Grescho, V., Harter, D., Jandt, U., May, R., Winter, M.,
884   & Jansen, F. (2021). Widespread decline in Central European plant diversity across six decades. *Global*
885   *Change Biology*, *27*(5), 1097–1110.

886 Essl, F., Dullinger, S., Genovesi, P., Hulme, P. E., Jeschke, J. M., Katsanevakis, S., Kühn, I., Lenzner, B.,
887   Pauchard, A., & Pyšek, P. (2019). A conceptual framework for range-expanding species that track
888   human-induced environmental change. *BioScience*, *69*(11), 908–919.

889 Ferrier, S., & Guisan, A. (2006). Spatial modelling of biodiversity at the community level. *Journal of Applied*
890   *Ecology, 43*(3), 393–404.

891 Finderup Nielsen, T., Sand-Jensen, K., Dornelas, M., & Bruun, H. H. (2019). More is less: Net gain in species
892   richness, but biotic homogenization over 140 years. *Ecology Letters*, *22*(10), 1650–1657.

893 Fitter, A. H., & Peat, H. J. (1994). The ecological flora database. *Journal of Ecology*, 415–425.

894 Freiberg, M., Winter, M., Gentile, A., Zizka, A., Muellner-Riehl, A. N., Weigelt, A., & Wirth, C. (2020). LCVP,
895   The Leipzig catalogue of vascular plants, a new taxonomic reference list for all known vascular plants.
896   *Scientific Data*, *7*(1), 1–7.

897   Garnier, E., Cortez, J., Billès, G., Navas, M. L., Roumet, C., Debussche, M., ... & Toussaint, J. P. (2004). Plant
898   functional markers capture ecosystem properties during secondary succession. *Ecology, 85*(9), 2630–
899   2637.
900   Gelman, A., & Rubin, D. B. (1992). Inference from iterative simulation using multiple sequences. *Statistical*
901   *Science*, *7*(4), 457–472.
902   Giulio, S., Acosta, A. T. R., Carboni, M., Campos, J. A., Chytrỳ, M., Loidi, J., Pergl, J., Pyšek, P., Isermann, M., &
903   Janssen, J. A. (2020). Alien flora across European coastal dunes. *Applied Vegetation Science*, *23*(3),
904   317–327.
905   Gross, N., Börger, L., Duncan, R. P., & Hulme, P. E. (2013). Functional differences between alien and native
906   species: Do biotic interactions determine the functional structure of highly invaded grasslands?
907   Functional Ecology, 27(5), 1262–1272.
908   Guo, J., Jiang, W., & Chen, G. (2020). Transient solute dispersion in wetland flows with submerged vegetation:
909   an analytical study in terms of time-dependent properties. *Water Resources Research*, *56*(2),
910   e2019WR025586.
911   Hanisch, M., Schweiger, O., Cord, A. F., Volk, M., & Knapp, S. (2020). Plant functional traits shape multiple
912   ecosystem services, their trade-offs and synergies in grasslands. *Journal of Applied Ecology, 57*(8),
913   1535–1550.
914   Hanz, D. M., Cutts, V., Barajas‐Barbosa, M. P., Algar, A. C., Beierkuhnlein, C., Fernández‐Palacios, J. M., ... &
915   Irl, S. D. (2022). Climatic and biogeographical drivers of functional diversity in the flora of the Canary
916   Islands. *Global Ecology and Biogeography*.
917   Heger, T., Bernard-Verdier, M., Gessler, A., Greenwood, A. D., Grossart, H. P., Hilker, M., Keinath, S.,
918   Kowarik, I., Kueffer, C., Marquard, E., Muller, J., Niemeier, S., Onandia, G., Petermann, J. S., Rillig, M.
919   C., Rodel, M. O., Saul, W. C., Schittko, C., Tockner, K., Joshi, J. & Jeschke, J. M. (2019) Towards an
920   Integrative, Eco-Evolutionary Understanding of Ecological Novelty: Studying and Communicating
921   Interlinked Effects of Global Change. *BioScience*, *69*, 888–899.
922   Henn, J. J., Yelenik, S., & Damschen, E. I. (2019). Environmental gradients influence differences in leaf
923   functional traits between native and non-native plants. *Oecologia*, *191*(2), 397–409.
924   Hijmans, R. J. (2021). Raster: Geographic Data Analysis and Modeling. R package version 3.4-13.
925   https://CRAN.R-project.org/package=raster.
926   Huang, S., Krysanova, V., & Hattermann, F. (2015). Projections of climate change impacts on floods and
927   droughts in Germany using an ensemble of climate change scenarios. *Regional Environmental Change*,
928   *15*(3), 461–473.
929   Hulme, P. E., & Bernard-Verdier, M. (2018a). Comparing traits of native and alien plants: Can we do better?
930   *Functional Ecology*, *32*(1), 117–125.
931   Hulme, P. E., & Bernard-Verdier, M. (2018b). Evaluating differences in the shape of native and alien plant trait
932   distributions will bring new insights into invasions of plant communities. *Journal of Vegetation*
933   *Science*, *29*(2), 348–355.
934   Jansen, F., & Dengler, J. (2008). GermanSL – eine universelle taxonomische Referenzliste für
935   Vegetationsdatenbanken. *Tuexenia*, *28*, 239–253.
936   Jansen, F., & Dengler, J. (2010). Plant names in vegetation databases–a neglected source of bias. *Journal of*
937   *Vegetation Science*, *21*(6), 1179–1186.

938 Joswig, J. S., Wirth, C., Schuman, M. C., Kattge, J., Reu, B., Wright, I. J., ... & Mahecha, M. D. (2022). Climatic
939   and soil factors explain the two-dimensional spectrum of global plant trait variation. *Nature Ecology &*
940   *Evolution, 6*(1), 36–50.

941 Kalusová, V., Čeplová, N. & Lososová, Z. (2017). Which traits influence the frequency of plant species
942   occurrence in urban habitat types?. *Urban Ecosystems 20*, 65–75.

943 Kaplan, Z., Danihelka, J., Chrtek, J. Jr., Kirschner, J., Kubát, K., Štěpánek, J., & Štech, M. (eds) (2019) Klíč ke
944   květeně České republiky [Key to the flora of the Czech Republic]. Ed. 2. – Academia, Praha.

945 Kattge, J., Boenisch, G., Diaz, S., Lavorel, S., Prentice, I. C., Leadley, P., Tautenhahn, S., Werner, G. D. A.,
946   Aakala, T., Abedi, M., Acosta, A. T. R., Adamidis, G. C., Adamson, K., Aiba, M., Albert, C. H.,
947   Alcantara, J. M., Alcazar, C. C., Aleixo, I., Ali, H., … Wirth, C. (2020). TRY plant trait database—
948   Enhanced coverage and open access. *Global Change Biology*, *26*(1), 119–188.

949 Kattge, J., Diaz, S., Lavorel, S., Prentice, C., Leadley, P., Boenisch, G., Garnier, E., Westoby, M., Reich, P. B.,
950   Wright, I. J., Cornelissen, J. H. C., Violle, C., Harrison, S. P., van Bodegom, P. M., Reichstein, M.,
951   Enquist, B. J., Soudzilovskaia, N. A., Ackerly, D. D., Anand, M., … Wirth, C. (2011). TRY - a global
952   database of plant traits. *Global Change Biology*, *17*(9), 2905–2935.

953 Kleyer, M., Bekker, R. M., Knevel, I. C., Bakker, J. P., Thompson, K., Sonnenschein, M., Poschlod, P., Van
954   Groenendael, J. M., Klimeš, L., & Klimešová, J. (2008). The LEDA Traitbase: A database of life-history
955   traits of the Northwest European flora. *Journal of Ecology*, *96*(6), 1266–1274.

956 Klimešová, J., Mudrák, O., Martínková, J., Lisner, A., Lepš, J., Filartiga, A. L., & Ottaviani, G. (2021). Are
957   belowground clonal traits good predictors of ecosystem functioning in temperate grasslands?.
958   *Functional Ecology, 35*(3), 787–795.

959 Knapp, S., & Kühn, I. (2012). Origin matters: Widely distributed native and non-native species benefit from
960   different functional traits. *Ecology Letters*, *15*(7), 696–703.

961 Kok, K., Pedde, S., Gramberger, M., Harrison, P. A., & Holman, I. P. (2019). New European socio-economic
962   scenarios for climate change research: Operationalising concepts to extend the shared socio-economic
963   pathways. *Regional Environmental Change*, *19*(3), 643–654.

964 Krkoška Lorencová, E., Whitham, C. E., Bašta, P., Harmáčková, Z. V., Štěpánek, P., Zahradníček, P., Farda, A.,
965   & Vačkář, D. (2018). Participatory climate change impact assessment in three Czech cities: The case of
966   heatwaves. *Sustainability*, *10*(6), 1906.

967 Kühn, I., Durka, W., & Klotz, S. (2004). BiolFlor: A new plant-trait database as a tool for plant invasion ecology.
968   *Diversity and Distributions*, *10*(5/6), 363–365.

969 Kühn, N., Tovar, C., Carretero, J., Vandvik, V., Enquist, B. J., & Willis, K. J. (2021). Globally important plant
970   functional traits for coping with climate change. *Frontiers of Biogeography*, *13*(4), e53774.

971 Küster, E. C., Bierman, S. M., Klotz, S., & Kühn, I. (2011). Modelling the impact of climate and land use change
972   on the geographical distribution of leaf anatomy in a temperate flora. *Ecography*, *34*(3), 507–518.

973 Küster, E. C., Kühn, I., Bruelheide, H., & Klotz, S. (2008). Trait interactions help explain plant invasion success
974   in the German flora. *Journal of Ecology*, *96*(5), 860–868.

975 Kunstler, G., Falster, D., Coomes, D. A., Hui, F., Kooyman, R. M., Laughlin, D. C., ... & Westoby, M. (2016).
976   Plant functional traits have globally consistent effects on competition. *Nature, 529*(7585), 204–207.

977 Lavorel, S., & Garnier, E. (2002). Predicting changes in community composition and ecosystem functioning
978   from plant traits: Revisiting the Holy Grail. *Functional Ecology*, *16*(5), 545–556.

979 Liu, Y., Oduor, A. M. O., Zhang, Z., Manea, A., Tooth, I. M., Leishman, M. R., Xu, X., & Kleunen, M. van.
980   (2017). Do invasive alien plants benefit more from global environmental change than native plants?
981   *Global Change Biology*, *23*(8), 3363–3370.
982 Madani, N., Kimball, J. S., Ballantyne, A. P., Affleck, D. L., Van Bodegom, P. M., Reich, P. B., Kattge, J., Sala, A.,
983   Nazeri, M., & Jones, M. O. (2018). Future global productivity will be affected by plant trait response to
984   climate. *Scientific Reports*, *8*(1), 1–10.
985 Maes, S. L., Perring, M. P., Depauw, L., Bernhardt-Römermann, M., Blondeel, H., Brūmelis, G., Brunet, J.,
986   Decocq, G., den Ouden, J., & Govaert, S. (2020). Plant functional trait response to environmental
987   drivers across European temperate forest understorey communities. *Plant Biology*, *22*(3), 410–424.
988 Maron, J. L., Vila, M., Bommarco, R., Elmendorf, S., & Beardsley, P. (2004). Rapid evolution of an invasive
989   plant. *Ecological Monographs*, *74*, 261–280.
990 Mathakutha, R., Steyn, C., le Roux, P. C., Blom, I. J., Chown, S. L., Daru, B. H., Ripley, B. S., Louw, A., & Greve,
991   M. (2019). Invasive species differ in key functional traits from native and non-invasive alien plant
992   species. *Journal of Vegetation Science*, *30*(5), 994–1006.
993 McGill, B. J., Enquist, B. J., Weiher, E., & Westoby, M. (2006). Rebuilding community ecology from functional
994   traits. *Trends in Ecology & Evolution*, *21*(4), 178–185.
995 Milanović, M., Knapp, S., Pyšek, P., & Kühn, I. (2020). Trait–environment relationships of plant species at
996   different stages of the introduction process. *NeoBiota*, *58*, 55.
997 Moles, A. T. (2018). Being John Harper: Using evolutionary ideas to improve understanding of global patterns in
998   plant traits. *Journal of Ecology*, *106*(1), 1–18.
999 Moles, A. T., Perkins, S. E., Laffan, S. W., Flores-Moreno, H., Awasthy, M., Tindall, M. L., Sack, L., Pitman, A.,
1000   Kattge, J., & Aarssen, L. W. (2014). Which is a better predictor of plant traits: Temperature or
1001   precipitation? *Journal of Vegetation Science*, *25*(5), 1167–1180.
1002 Moles, A. T., Warton, D. I., Warman, L., Swenson, N. G., Laffan, S. W., Zanne, A. E., Pitman, A., Hemmings, F.
1003   A., & Leishman, M. R. (2009). Global patterns in plant height. *Journal of Ecology*, *97*(5), 923–932.
1004 Musavi, T., Migliavacca, M., van de Weg, M. J., Kattge, J., Wohlfahrt, G., van Bodegom, P. M., ... & Mahecha,
1005   M. D. (2016). Potential and limitations of inferring ecosystem photosynthetic capacity from leaf
1006   functional traits. *Ecology and evolution, 6*(20), 7352–7366.
1007 Myers-Smith, I. H., Thomas, H. J. D., & Bjorkman, A. D. (2019). Plant traits inform predictions of tundra
1008   responses to global change. *New Phytologist*, *221*(4), 1742–1748.
1009 Naeem, S., Duffy, J. E., & Zavaleta, E. (2012). The functions of biological diversity in an age of extinction.
1010   *Science*, *336*(6087), 1401–1406.
1011 Naimi, B., Hamm, N. A., Groen, T. A., Skidmore, A. K., & Toxopeus, A. G. (2014). Where is positional
1012   uncertainty a problem for species distribution modelling? *Ecography*, *37*(2), 191–203.
1013 NetPhyD & BfN (Netzwerk Phytodiversität Deutschlands e.V. & Bundesamt für Naturschutz) (2013).
1014   Verbreitungsatlas der Farn- und Blütenpflanzen Deutschlands. pp 912. Bundesamt für Naturschutz,
1015   Bonn - Bad Godesberg.
1016 New, M., Lister, D., Hulme, M., & Makin, I. (2002). A high-resolution data set of surface climate over global
1017   land areas. *Climate Research*, *21*, 1–25.
1018 Oksanen, J., Blanchet, F. G., Friendly, M., Kindt, R., ... Legendre, P. (2020). *Vegan: Community Ecology*
1019   *Package. R package version 2.5-7. Https://CRAN.R-project.org/package=vegan*.

1020 Ordonez, J. C., van Bodegom, P. M., Witte, J.-P. M., Wright, I. J., Reich, P. B., & Aerts, R. (2009). A global
1021   study of relationships between leaf traits, climate and soil measures of nutrient fertility. *Global Ecology*
1022   *and Biogeography*, *18*(2), 137–149. https://doi.org/10.1111/j.1466-8238.2008.00441.x
1023 Pollock, L. J., Morris, W. K., & Vesk, P. A. (2012). The role of functional traits in species distributions revealed
1024   through a hierarchical model. *Ecography*, *35*(8), 716–725.
1025 POWO (2022). Plants of the World Online. Facilitated by the Royal Botanic Gardens, Kew. Published on the
1026   Internet; http://www.plantsoftheworldonline.org/ Retrieved February 2022.
1027 Pyšek, P., Hulme, P. E., Simberloff, D., Bacher, S., Blackburn, T. M., Carlton, J. T., Dawson, W., Essl, F.,
1028   Foxcroft, L. C., & Genovesi, P. (2020). Scientists' warning on invasive alien species. *Biological Reviews*,
1029   *95*(6), 1511–1534.
1030 Pyšek, P., & Richardson, D. M. (2008). Traits associated with invasiveness in alien plants: Where do we stand?
1031   In Biological invasions (pp. 97–125). Springer.
1032 R Core Team (2021). R: A language and environment for statistical computing. R Foundation for Statistical
1033   Computing, Vienna, Austria. URL https://www.R-project.org/.
1034 Roberts, D. R., Bahn, V., Ciuti, S., Boyce, M. S., Elith, J., Guillera-Arroita, G., Hauenstein, S., Lahoz-Monfort, J.
1035   J., Schröder, B., & Thuiller, W. (2017). Cross-validation strategies for data with temporal, spatial,
1036   hierarchical, or phylogenetic structure. *Ecography*, *40*(8), 913–929.
1037 Rosbakh, S., Römermann, C., & Poschlod, P. (2015). Specific leaf area correlates with temperature: New
1038   evidence of trait variation at the population, species and community levels. *Alpine Botany*, *125*(2), 79–
1039   86.
1040 Roy, D., Alderman, P., Arianoutsou, M., … Augustin, S. (2020). *DAISIE - Inventory of alien invasive species in*
1041   *Europe. Version 1.7.* Research Institute for Nature and Forest (INBO). Checklist dataset
1042   https://doi.org/10.15468/ybwd3x
1043 Rulfová, Z., Beranová, R., & Kyselỳ, J. (2017). Climate change scenarios of convective and large-scale
1044   precipitation in the Czech Republic based on EURO-CORDEX data. *International Journal of*
1045   *Climatology*, *37*(5), 2451–2465.
1046 Sádlo, J., Chytrý, M., & Pyšek, P. (2007) Regional species pools of vascular plants in habitats of the Czech
1047   Republic. *Preslia, 79*, 303–321.
1048 Sandel, B., Goldstein, L. J., Kraft, N. J. B., Okie, J. G., Shuldman, M. I., Ackerly, D. D., Cleland, E. E., & Suding,
1049   K. N. (2010). Contrasting trait responses in plant communities to experimental and geographic
1050   variation in precipitation. *New Phytologist*, *188*(2), 565–575.
1051 Sandel, B., & Low, R. (2019). Intraspecific trait variation, functional turnover and trait differences among native
1052   and exotic grasses along a precipitation gradient. *Journal of Vegetation Science, 30*(4), 633–643.
1053 Saul, W.-C., Jeschke, J., & Heger, T. (2013). The role of eco-evolutionary experience in invasion success.
1054   *NeoBiota, 17*, 57–74.
1055 Seebens, H., Blackburn, T. M., Dyer, E. E., Genovesi, P., Hulme, P. E., Jeschke, J. M., Pagad, S., Pyšek, P.,
1056   Winter, M., & Arianoutsou, M. (2017). No saturation in the accumulation of alien species worldwide.
1057   *Nature Communications*, *8*(1), 1–9.
1058 Šímová, I., Violle, C., Kraft, N. J. B., Storch, D., Svenning, J.-C., Boyle, B., Donoghue, J. C., Jørgensen, P.,
1059   McGill, B. J., Morueta-Holme, N., Piel, W. H., Peet, R. K., Regetz, J., Schildhauer, M., Spencer, N.,
1060   Thiers, B., Wiser, S., & Enquist, B. J. (2015). Shifts in trait means and variances in North American tree

1061   assemblages: Species richness patterns are loosely related to the functional space. *Ecography*, *38*(7),
1062   649–658.
1063 Šímová, I., Violle, C., Svenning, J.-C., Kattge, J., Engemann, K., Sandel, B., Peet, R. K., Wiser, S. K., Blonder, B.,
1064   & McGill, B. J. (2018). Spatial patterns and climate relationships of major plant traits in the New World
1065   differ between woody and herbaceous species. *Journal of Biogeography*, *45*(4), 895–916.
1066 Štěpánek, P., Zahradníček, P., Farda, A., Skalák, P., Trnka, M., Meitner, J., & Rajdl, K. (2016). Projection of
1067   drought-inducing climate conditions in the Czech Republic according to Euro-CORDEX models.
1068   *Climate Research*, *70*(2–3), 179–193.
1069 Swenson, N. G., Enquist, B. J., Pither, J., Kerkhoff, A. J., Boyle, B., Weiser, M. D., Elser, J. J., Fagan, W. F.,
1070   Forero-Montaña, J., Fyllas, N., Kraft, N. J. B., Lake, J. K., Moles, A. T., Patiño, S., Phillips, O. L., Price,
1071   C. A., Reich, P. B., Quesada, C. A., Stegen, J. C., … Nolting, K. M. (2012). The biogeography and
1072   filtering of woody plant functional diversity in North and South America. *Global Ecology and*
1073   *Biogeography*, *21*(8), 798–808.
1074 Taseski, G. M., Beloe, C. J., Gallagher, R. V., Chan, J. Y., Dalrymple, R. L., & Cornwell, W. K. (2019). A global
1075   growth-form database for 143,616 vascular plant species. *Ecology, 100*(3), e02614.
1076 Thuiller, W., Guéguen, M., Renaud, J., Karger, D. N., & Zimmermann, N. E. (2019). Uncertainty in ensembles
1077   of global biodiversity scenarios. *Nature Communications*, *10*(1), 1446.
1078 Thuiller, W., Lavorel, S., Araújo, M. B., Sykes, M. T., & Prentice, I. C. (2005). Climate change threats to plant
1079   diversity in Europe. *Proceedings of the National Academy of Sciences*, *102*(23), 8245–8250.
1080 Valavi, R., Elith, J., Lahoz-Monfort, J. J., & Guillera-Arroita, G. (2019). blockCV: An r package for generating
1081   spatially or environmentally separated folds for k-fold cross-validation of species distribution models.
1082   *Methods in Ecology and Evolution*, *10*(2), 225–232.
1083 van Kleunen, M., Weber, E., & Fischer, M. (2010). A meta-analysis of trait differences between invasive and
1084   non-invasive plant species. *Ecology Letters*, *13*(2), 235–245.
1085 Vandelook, F., Janssens, S. B., & Matthies, D. (2018). Ecological niche and phylogeny explain distribution of
1086   seed mass in the central European flora. *Oikos*, *127*(10), 1410–1421.
1087 Violle, C., Navas, M. L., Vile, D., Kazakou, E., Fortunel, C., Hummel, I., & Garnier, E. (2007). Let the concept of
1088   trait be functional!. *Oikos, 116*(5), 882–892.
1089 Violle, C., Reich, P. B., Pacala, S. W., Enquist, B. J., & Kattge, J. (2014). The emergence and promise of
1090   functional biogeography. *Proceedings of the National Academy of Sciences*, *111*(38), 13690–13696.
1091 Vojtkó, A. E., Balogh, N., Deák, B., Kelemen, A., Kis, S., Kiss, R., Lovas-Kiss, Á., Löki, V., Lukács, K., Molnár V,
1092   A., & Nagy, T. (2020). Leaf trait records of vascular plant species in the Pannonian flora with special
1093   focus on endemics and rarities. *Folia Geobotanica*, *55*(2), 73–79.
1094 Wagner, V., Chytrỳ, M., Jiménez-Alfaro, B., Pergl, J., Hennekens, S., Biurrun, I., Knollová, I., Berg, C., Vassilev,
1095   K., & Rodwell, J. S. (2017). Alien plant invasions in European woodlands. *Diversity and Distributions*,
1096   *23*(9), 969–981.
1097 Wellstein, C., Poschlod, P., Gohlke, A., Chelli, S., Campetella, G., Rosbakh, S., Canullo, R., Kreyling, J., Jentsch,
1098   A., & Beierkuhnlein, C. (2017). Effects of extreme drought on specific leaf area of grassland species: A
1099   meta-analysis of experimental studies in temperate and sub-Mediterranean systems. *Global Change*
1100   *Biology*, *23*(6), 2473–2481.
1101 Wesner, J. S., & Pomeranz, J. P. (2021). Choosing priors in Bayesian ecological models by simulating from the
1102   prior predictive distribution. *Ecosphere*, *12*(9), e03739.

1103   Westerband, A. C., Knight, T. M., & Barton, K. E. (2020). Intraspecific trait variation and reversals of trait
1104   strategies across key climate gradients in native Hawaiian plants and non-native invaders. *Annals of*
1105   *Botany*, *127*(4), 553–564.
1106   Westoby, M. (1998). A leaf-height-seed (LHS) plant ecology strategy scheme. *Plant and Soil*, *199*(2), 213–227.
1107   Wieczynski, D. J., Boyle, B., Buzzard, V., Duran, S. M., Henderson, A. N., Hulshof, C. M., Kerkhoff, A. J.,
1108   McCarthy, M. C., Michaletz, S. T., & Swenson, N. G. (2019). Climate shapes and shifts functional
1109   biodiversity in forests worldwide. *Proceedings of the National Academy of Sciences*, *116*(2), 587–592.
1110   Wild, J., Kaplan, Z., Danihelka, J., Petřík, P., Chytrý, M., Novotný, P., Rohn, M., Šulc, V., Brůna, J., Chobot, K.,
1111   Ekrt, L., Holubová, D., Knollová, I., Kocián, P., Štech, M., Štěpánek, J., & Zouhar, V. (2019). Plant
1112   distribution data for the Czech Republic integrated in the Pladias database. *Preslia*, *91*(1), 1–24.
1113   Winter, M., Schweiger, O., Klotz, S., Nentwig, W., Andriopoulos, P., Arianoutsou, M., Basnou, C., Delipetrou,
1114   P., Didžiulis, V., & Hejda, M. (2009). Plant extinctions and introductions lead to phylogenetic and
1115   taxonomic homogenization of the European flora. *Proceedings of the National Academy of Sciences*,
1116   *106*(51), 21721–21725.
1117   Wright, I. J., Reich, P. B., Cornelissen, J. H. C., Falster, D. S., Groom, P. K., Hikosaka, K., Lee, W., Lusk, C. H.,
1118   Niinemets, Ü., Oleksyn, J., Osada, N., Poorter, H., Warton, D. I., & Westoby, M. (2005). Modulation of
1119   leaf economic traits and trait relationships by climate. *Global Ecology and Biogeography*, *14*(5), 411–
1120   421.
1121   Wright, I. J., Reich, P. B., Westoby, M., Ackerly, D. D., Baruch, Z., Bongers, F., ... & Villar, R. (2004). The
1122   worldwide leaf economics spectrum. *Nature, 428*(6985), 821–827.
1123   Yang, Q., Weigelt, P., Fristoe, T. S., Zhang, Z., Kreft, H., Stein, A., ... & van Kleunen, M. (2021). The global loss
1124   of floristic uniqueness. *Nature communications, 12*(1), 1–10.
1125   Yao, Y., Vehtari, A., Simpson, D., & Gelman, A. (2018). Using stacking to average Bayesian predictive
1126   distributions (with discussion). *Bayesian Analysis*, *13*(3), 917–1007.
1127   Zanne, A. E., Tank, D. C., Cornwell, W. K., Eastman, J. M., Smith, S. A., FitzJohn, R. G., McGlinn, D. J.,
1128   O'Meara, B. C., Moles, A. T., & Reich, P. B. (2014). Three keys to the radiation of angiosperms into
1129   freezing environments. *Nature*, *506*(7486), 89–92.

1130   **FIGURES**

1131

1132   FIGURE 1

1133   The projected absolute overall per-cell change across the three traits, plant maximum height

1134   (H_{max}), specific leaf area (SLA), and seed mass (SM), at the habitat (a), biogeographical status

1135   (b), and woodiness (c) levels under the least extreme combined climate and socio-economic

1136   scenario (RCP2.6 Eur-SSP1, all climate models pooled) and the most extreme one (RCP8.5

1137   Eur-SSP5) for 2081–2100. The overall trait change was calculated as a Euclidean distance

1138   between projected per-cell posterior means of the three traits on baseline data and scenario

1139   data. Boxes show 25%, 50%, and 75% quartiles, and whiskers show 95% credible intervals.

1140

1141   FIGURE 2

1142   The projected per-cell (10' × 10') change in the $\log_{10}$-transformed maximum plant height

1143   (H_{max}) under the least extreme combined climate and socio-economic scenario (RCP2.6 Eur-

1144   SSP1, all climate models pooled) and the most extreme one (RCP8.5 Eur-SSP5) for 2081–

1145   2100, for herbaceous (a, c) and woody (b, d) taxa in six broad habitat types. The trait change

1146   here is expressed as the posterior means of per-cell model predictions. The violin plots depict

1147   the distributions of predicted values across the study area and climate models (Table S1) and

1148   the boxplots provide summary statistics of those distributions (boxes show 25%, 50%, and

1149   75% quartiles and whiskers give roughly 95% credible intervals). For each habitat by

1150   woodiness combination, the trait change is presented in standard deviations (SD) of the

1151   baseline trait distribution of native taxa for that combination. For example, the overall

1152   change of 0.60 in H_{max} of forest herbaceous neophytes under the RCP2.6 Eur-SSP1 scenario

1153   indicates that the average H_{max} of this assemblage is projected to increase by 0.60 SD, relative

1154   to the current H_{max} distribution of natives. Note the different scaling of Y-axes. Projections

1155   under other scenarios are illustrated in Figures S2, S3 (projected per-cell posterior means),

1156   S8, S9 (projected per-cell posterior standard deviations).

1157

1158   FIGURE 3

1159   The projected per-cell (10' × 10') change in the $\log_{10}$-transformed specific leaf area (SLA)

1160   under the least extreme combined climate and socio-economic scenario (RCP2.6 Eur-SSP1,

1161   all climate models pooled) and the most extreme one (RCP8.5 Eur-SSP5) for herbaceous (a, c)

1162   and woody (b, d) taxa in six broad habitat types. Projections under other scenarios are

1163   illustrated in Figures S4, S5 (projected per-cell posterior means), S10, S11 (projected per-cell

1164   posterior standard deviations). Other details are as in Figure 2.

1165

1166   FIGURE 4

1167   The projected per-cell (10' × 10') change in the $\log_{10}$-transformed plant seed mass (SM) under

1168   the least extreme combined climate and socio-economic scenario (RCP2.6 Eur-SSP1, all

1169   climate models pooled) and the most extreme one (RCP8.5 Eur-SSP5) for 2081–2100, for

1170   herbaceous (a, c) and woody (b, d) taxa in six broad habitat types. Projections under other

1171   scenarios are illustrated in Figures S6, S7 (projected per-cell posterior means), S12, and S13

1172   (projected per-cell posterior standard deviations). Other details are as in Figure 2.

1173

1174   FIGURE 5

1175   The relative contribution of individual environmental predictors to the projected change in

1176   herbaceous (a–r) and woody (s–x) plant maximum height (H_{max}), specific leaf area (SLA), and

1177   seed mass (SM), calculated using redundancy analysis (RDA). A separate RDA was performed

1178   on each subset ($N = 24$) of per-cell projections across all the scenarios, representing a unique

1179   combination of taxon biogeographical status, habitat, and woodiness. Shown are the RDA

1180   scores of the predictors (as vectors) and traits (as triangles; centered at seed mass) for the two

1181   first RDA axes (RDA1, RDA2). RDA1 and RDA2 together captured 91–100% of the variation

1182   in the data. The lengths of vectors are proportional to the magnitude of the effects of

1183   respective predictors on the three traits simultaneously. The overall contributions of each

1184   predictor, calculated as the combined length of respective vectors across all the RDA spaces,

1185   are shown in Figure S18. The angles among the vectors and triangles reflect their correlation,

1186   which equals the cosine of the angle. For example, the angle between SM and precipitation

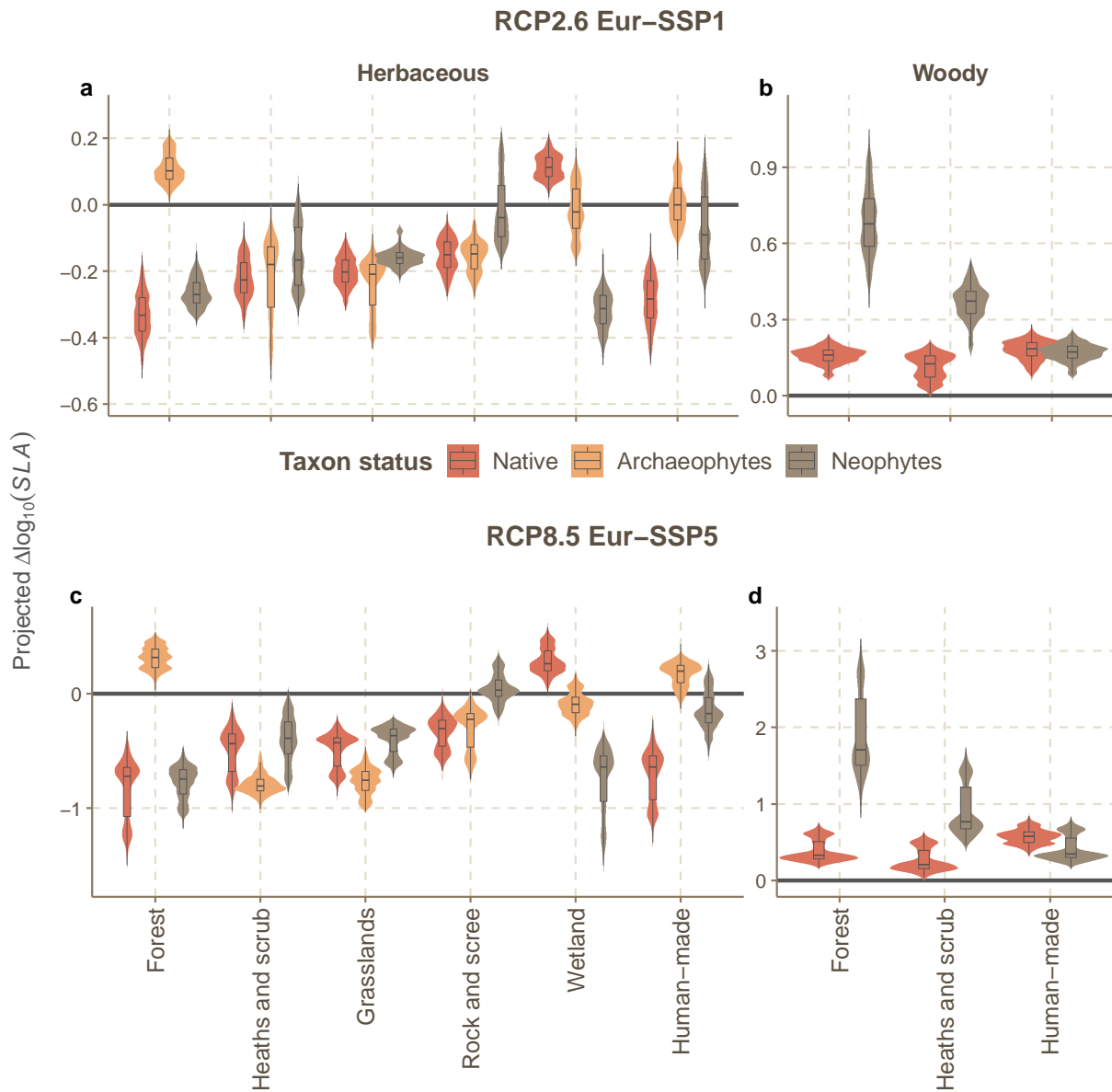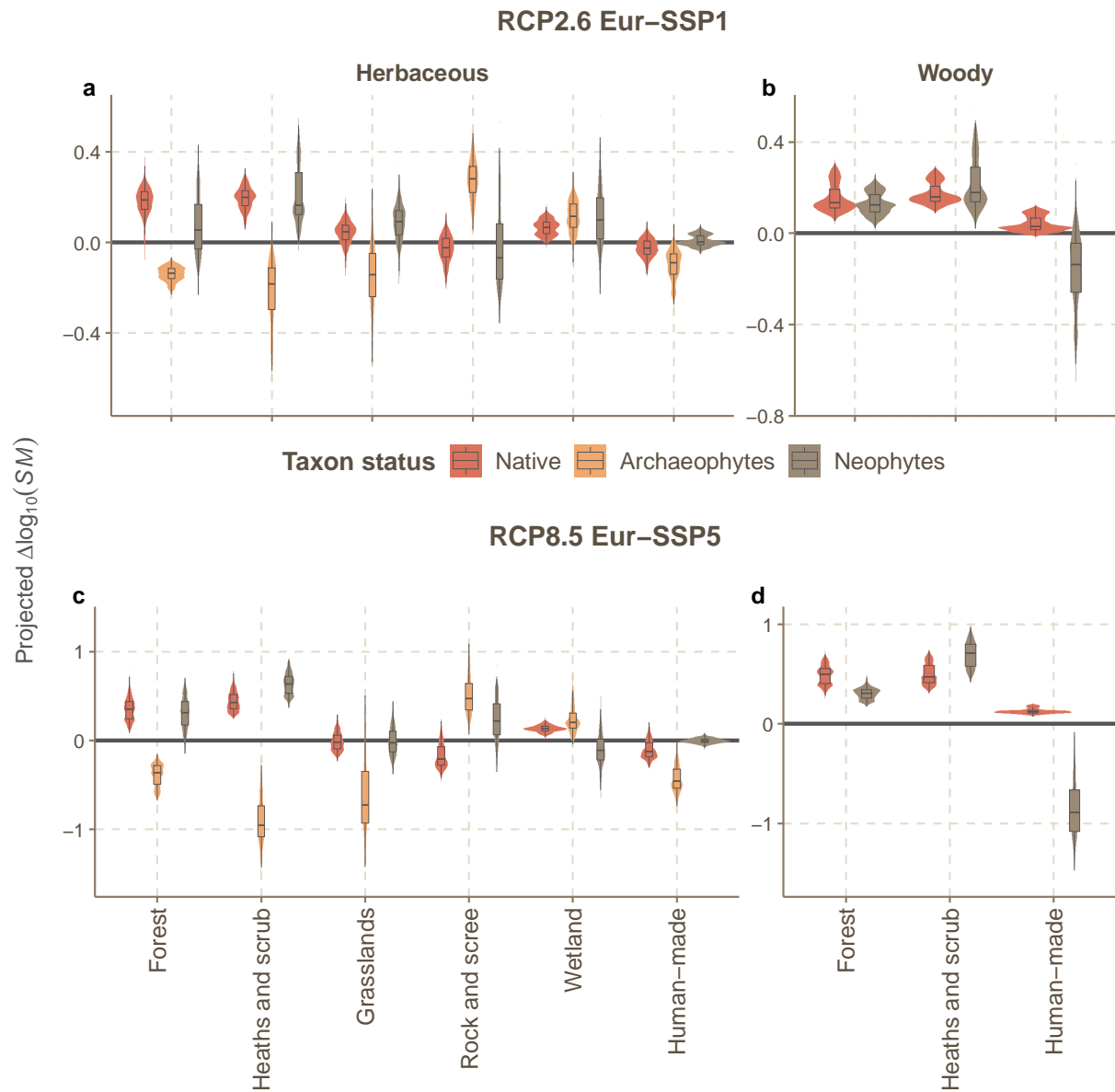1187   seasonality is acute for most assemblages, indicating their strong positive correlation.

1188
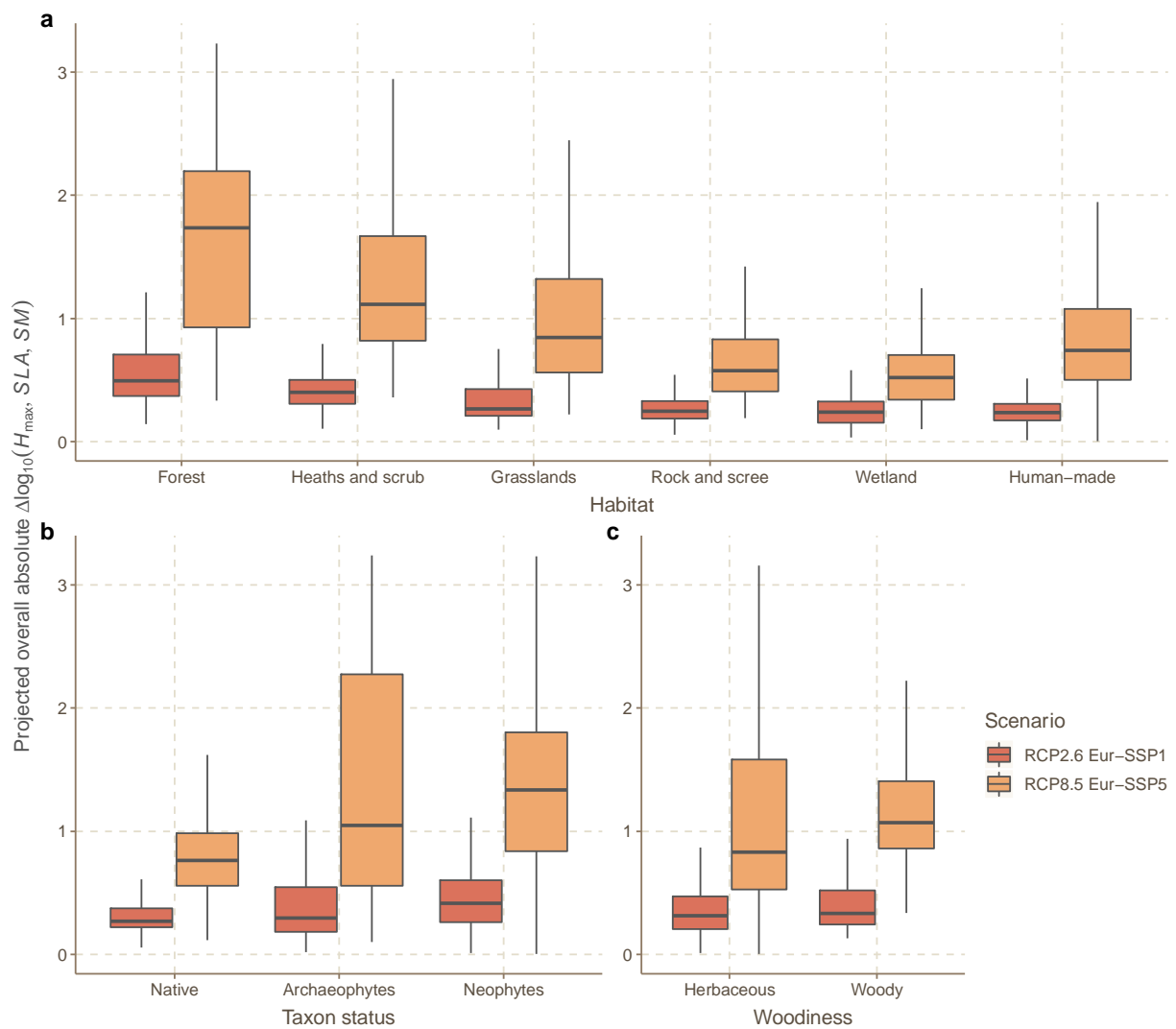
1189
1190
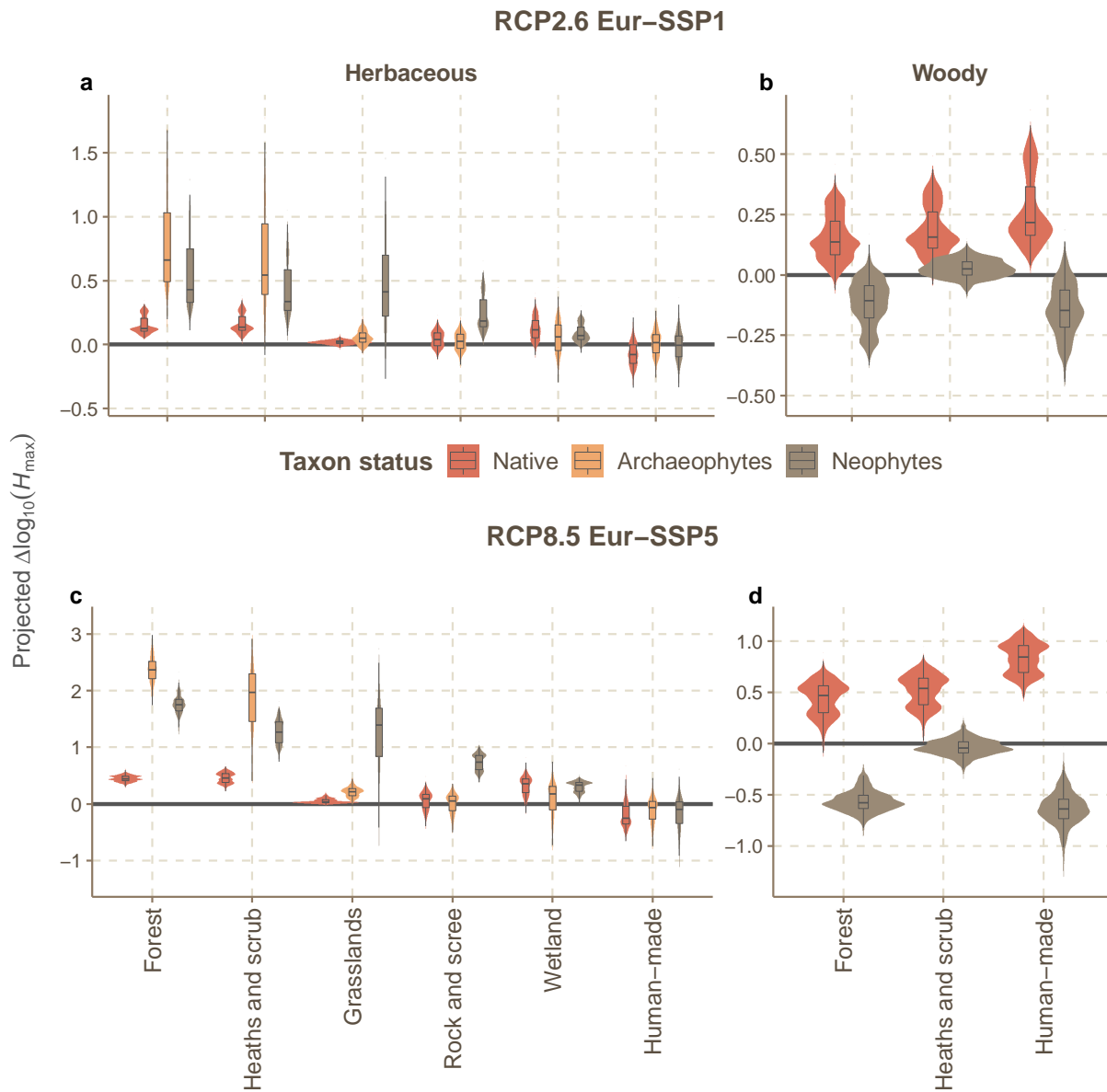
1191
1192

1193
1194

1195
1196

1197